TARGETING IN CHAOS USING ANALYTICALLY DESCRIBED CLUSTERS

by

Yağız Sütçü

B.S. in Industrial Engineering,

Galatasaray University, 1998

Submitted to the Institute for Graduate Studies in

Science and Engineering in partial fulfillment of

the requirements for the degree of

Master of Science

in

Systems and Control Engineering

Boğaziçi University

2002

ACKNOWLEDGEMENTS

First of all, I am deeply grateful to my thesis supervisor, Assoc. Prof. Yağmur DENİZHAN for his academic support and friendly tolerance.

I also deeply appreciate the invaluable assistance provided by Serdar İPLİKÇİ. I am extremely grateful for his practice and collaboration.

I wish to thank also Assist. Prof. Sedat ŞİŞBOT, who supported me in my thesis and whose support gave me spiritual strength in pursuing my ambition.

Thanks go to all my friends and especially to Mesut Ali ERGİN who assisted me without request and was very helpful in his suggestions.

A special thank you goes to my parents who always supported me in my plans and studies.

Lastly, I want to send my thanks and my love to Nevin, who was always there for me.

ABSTRACT

TARGETING IN CHAOS USING ANALYTICALLY DESCRIBED CLUSTERS

The OGY method provides a simple but powerful approach of controlling chaotic dynamics. This method can stabilise inherently unstable equilibrium modes of dissipative chaotic systems under the lack of knowledge about the system equations. However, it has the typical drawback of a long waiting time until the system starting from random initial conditions enters the close neighbourhood of the equilibrium mode to be stabilised, where the controller can be activated. The reduction of this drawback is known under the name of targeting.

The Extended Control Regions method is a targeting approach, which can operate under the lack of knowledge about the system equations by employing local models of the system dynamics extracted from empirical data. The method is based on the idea of identifying and modelling those regions of the phase space, starting from which the system can be steered to a close neighbourhood of the target within a few steps applying small perturbations in the control parameters. So far, the modelling of the system dynamics within these phase space regions have been realised using artificial neural networks.

In this study, two different strategies are developed in order to realise the clustered version of the Extended Control Regions method on basis of simple analytical models rather than neural networks. Each cluster obtained from the gathered data is analytically described as a hyper-ellipsoid. Subsequently, the analytical models of the clusters are used for targeting purposes by applying small discrete variations in the control parameter.

Simulation results on several chaotic systems with single control parameter show that the proposed method can achieve targeting using less memory and computation time than the Clustered Extended Control Regions method on cost of a slower targeting performance.

ÖZET

ANALİTİK OLARAK BETİMLENMİŞ KÜMELER YARDIMIYLA KAOTİK SİSTEMLERİN HEDEFE YÖNELTİLMESİ

OGY yöntemi, kaotik sistemlerin kontrolü için basit, ancak güçlü bir yaklaşım sunmakta ve enerji tüketen kaotik sistemlerin orijinalde kararsız olan denge modlarını, sistem denklemlerini bilmeksizin kararlı hale getirebilmektedir. Ancak, bu yöntemin en tipik dezavantajı, rastgele bir başlangıç noktasından başlandığında, sistemin kararlı hale getirilecek denge modu civarına oldukça uzun sürede yaklaşabilmesi ve sadece denge modu civarında kullanılabilen denetleyicinin oldukça geç devreye girmesidir. Bu dezavantajı azaltma çalışmaları, literatürde hedefe yöneltme olarak adlandırılmaktadır.

Genişletilmiş Denetim Bölgeleri yöntemi, deneysel verilerden elde edilen yerel modelleri kullanarak, sistem denklemlerinin bilinmediği durumlarda da çalışabilen bir hedefe yöneltme yaklaşımıdır. Bu yöntem, denetim parametrelerine küçük değişimler uygulayarak, sistemin hedef civarına bir kaç adımda yönlendirilebildiği çıkış bölgelerini belirleyip modelleme düşüncesine dayanmaktadır. Bugüne kadar, bu çıkış bölgelerindeki sistem dinamiğinin modellenmesi, yapay sinir ağları yardımıyla gerçekleştirilmiştir.

Bu çalışmada, Genişletilmiş Denetim Bölgeleri yönteminin kümelendirilmiş versiyonunun sinir ağları yerine, basit analitik modellerle gerçekleştirilmesini sağlayan iki farklı strateji geliştirilmiştir. Farklı metotlarla toplanan verilerden elde edilen alt-kümeler, analitik olarak bir hiper-elipsoid olarak modellenmekte; ardından bu modeller kullanılarak, denetleme parametresinde küçük ayrıksı oynamalarla sistem hedefe yöneltilmektedir.

Tek denetim parametreli çeşitli kaotik sistemler üzerinde yapılan benzetim sonuçları, önerilen yöntemin Kümelendirilmiş Genişletilmiş Denetim Bölgeleri yönteminden daha az bellek ve işlem süresi ile ancak daha düşük hızla hedefe yöneltmeyi gerçekleştirebildiğini, göstermiştir.

TABLE OF CONTENTS

ACKNOWLEDGEMENTS iii
ABSTRACT iv
ÖZET v
LIST OF FIGURES viii
LIST OF TABLES x
LIST OF SYMBOLS / ABBREVIATIONS xi
1. INTRODUCTION 1
2. INTRODUCTION TO DYNAMIC SYSTEMS AND THE RELEVANT MATHEMATICAL CONCEPTS 3
2.1. Dynamic Systems 3
2.2. Basic Concepts of Chaotic Dynamics 4
2.3. Discrete Representations of Continuous Dynamics and Determination of UPOs 7
2.4. Lyapunov's Linearisation Method and Extraction of the Local Linear Model 9
2.5. Delay Coordinates Method 10
3. OGY CONTROL AND TARGETING 12
3.1. Basic OGY Method 12
3.2. Targeting 16
4. ANALYTICALLY MODELLED CLUSTERS METHOD 18
4.1. Introduction 18
4.2. Extended Control Regions Method (ECR) 19
4.3. Main Idea of the Analytically Modelled Clusters (AMC) Method 20
4.4. Data Clustering 25
4.5. The Clustering Algorithm Used in the AMC Method 25
4.6. Application of the AMC Methods 27
4.6.1. Off-line Phase of the AMC-I Method 27
4.6.2. Off-line Phase of the AMC-II Method 28
4.6.3. Control Phase of the AMC Methods 30

5. SIMULATION RESULTS 34
5.1. Investigated Chaotic Systems. 34
5.1.1. The Logistic Map 34
5.1.2. The Hénon Map. 35
5.1.3 The Lorenz System 35
5.1.4. The Double Rotor Map. 36
5.2. Simulation Results. 37
6. CONCLUSION. 41
REFERENCES. 43

LIST OF FIGURES

Figure 2.1. Examples of regular (a),(b) and strange (c) attractors..... 7

Figure 2.2. Illustration of a Poincaré map..... 8

Figure 2.3. Different unstable periodic orbits of the Lorenz attractor..... 9

Figure 3.1. The idea of the OGY method..... 14

Figure 4.1. Control loop for targeting and control via neural networks..... 21

Figure 4.2. Illustration of the clustering algorithm used in AMC Methods..... 27

Figure 4.3. The idea of the AMC-I Method..... 29

Figure 4.4. Flow-charts describing off-line phases of (a) AMC-I and (b) AMC-II 30

Figure 4.5. Some clustered control regions determined for different chaotic systems..... 31

Figure 4.6. Data points belonging to first level control regions for (a) AMC-II and (b) AMC-I..... 32

Figure 4.7. The idea of the AMC-II method..... 32

Figure 4.8. On-line (control) phase of the AMC methods..... 33

Figure 5.1. Application of AMC-II Method to the Logistic map with 3 clustered control regions..... 38

LIST OF TABLES

Table 5.1. Comparison of OGY control and different versions of AMC methods for different chaotic systems..... 39

Table 5.2. Comparison of the OGY control and various ECR methods for different chaotic systems 40

LIST OF SYMBOLS / ABBREVIATIONS

A	Attractor
$\underline{\underline{A}}$	nxn Jacobian matrix of $\underline{f}$
$\underline{b}$	n-dimensional column vector
C_{ij}^{q}	Cluster of a control region
d_e	Delay map dimension
$\underline{f}$	Vector field
$\underline{F}$	Poincaré map
$\underline{G}, \underline{g}$	Discrete map
k	Index denoting discrete time steps
$\underline{\underline{N}}_{ij}^{q}$	Normalized Covariance Matrix of the cluster C_{ij}^{q}
$\underline{p}$	Control parameter vector
r	Radius of clustering
S_i^q	Control regions of the AMC-I Method
$\underline{s}$(t)	Delay coordinate vector
T_i^q	Control regions of the AMC-II Method
t	Continuous time
T	Delay time
U	Basin of attraction
$\underline{x}$	System state
$\underline{x}^*$	Equilibrium point
y(t)	Measurable variable
$\underline{z}^*$	Equilibrium point

$\underline{\mu}_{ij}^{q}$	Mean of cluster C_{ij}^{q}
Π_l, Π_q	Allowable range for control parameter change
δp_{max}	Maximum allowable parameter change for the control parameter
δ	Radius of the OGY region

AMC	Analytically Modelled Clusters
ECR	Extended Control Regions
NMD	Normalized Mahalanobis Distance
RBF	Radial Basis Function
UEP	Unstable Equilibrium Point
UPO	Unstable Periodic Orbit

1. INTRODUCTION

Many physical systems show sensitive dependence on initial conditions and behave in a long-term unpredictable manner for certain parameter regimes. This behaviour is referred to as chaos. A deterministic system is said to be *chaotic* whenever its evolution sensitively depends on the initial conditions. This property implies that two trajectories starting from two nearby initial conditions diverge exponentially in the course of time making long-term predictions of the system's behaviour impossible.

Modern studies of chaos started with Lorenz's work about modelling the convection in the atmosphere by computer simulations [1]. Due to a slight numerical error in initial conditions Lorenz accidentally discovered that a deterministic system could exhibit sensitive dependence on initial conditions. The fact that certain dynamical systems show such a critical dependence on initial conditions was known since the end of the last century. However, only in the last thirty years, experimental observations have showed that chaotic systems are common in nature. They can be found, for example, in Non-linear Optics (lasers), in Electronics (Chua-Matsumoto circuit), in Fluid Dynamics (Rayleigh-Bénard convection), in Chemistry (Belouzov-Zhabotinski reaction) and elsewhere. Many natural phenomena, which can be found in meteorology, the solar system, heart and brain of living organisms, can also be characterised as chaotic.

For many years, such a characteristic was considered as something to be strongly avoided, this made chaos undesirable. This problem has been first addressed by Ott, Grebogi and Yorke [2] and since then, gained much interest and found many important engineering, physical or medical applications.

The most important advantages of the OGY method and its extensions are the facts that, they do not require any *a priori* knowledge about the system dynamics and allow parameter-based-control with small control power expenditure. The OGY method is based on choosing one out of the rich repertoire of unstable equilibrium points and unstable periodic orbits as the desired behaviour and stabilising it using an empirically obtained local linear model. However, the major drawback of these methods is the usually long

waiting time until the system visits a close neighbourhood of the target where the local linear model is valid and the controller is activated. The problem of reducing this waiting time is referred to as the targeting problem in the literature.

Concerning real world applications which are influenced by noisy and non-stationary environments and where no analytical description in terms of a map or a vector field is available, an ideal, general targeting method for chaotic systems should have some basic features: It (1) should not require an analytical description of the system, (2) should be robust against noise and non-stationarity, (3) should allow the stabilisation of any unstable equilibrium point or unstable periodic orbit of any order, and (4) should offer the possibility of real time performance.

In the following chapter, basic concepts of dynamic system theory, the fundamental properties of chaotic systems and notation used will be reviewed. Also relevant mathematical concepts of chaotic dynamics will be considered.

In Chapter 3, the OGY Control Scheme, other OGY-Based control and targeting methods will be considered. In addition, main characteristics of these methods will be explained and some preliminary concepts used in the proposed method for targeting of chaotic systems will be introduced.

Chapter 4 presents the proposed methods in detail with an explanatory summary of another targeting method, namely Extended Control Regions (ECR) Method, which has inspired this study.

In Chapter 5, simulation results obtained from different chaotic systems will be presented and discussed. A comparison of different versions of the proposed method and a performance comparison between the proposed method and ECR methods will be given.

In the last chapter, interpretation of results, both weak and strong points of the proposed method will be summarised and future work and further possible improvements will be discussed.

2. INTRODUCTION TO DYNAMIC SYSTEMS AND THE RELEVANT MATHEMATICAL CONCEPTS

2.1. Dynamic Systems

Many physical systems can be well described in terms of finite-dimensional continuous-time dynamical systems. In this case the state $\underline{x}$ of the system depends only on a finite set of n state variables,

$$\underline{x}(t) = [x_1(t), x_2(t) \ldots x_n(t)]^T \in R^n \tag{2.1}$$

and the system dynamics can be expressed as a of first-order *non-autonomous ordinary vector differential equation*

$$\dot{\underline{x}}(t) = \underline{f}(\underline{x}(t), \underline{p}, t), \ \underline{x}(t) \in R^n, \ \underline{f} \in R^n \tag{2.2}$$

Still a large class of physical systems can also be described in terms of first-order *autonomous ordinary vector differential equations*

$$\dot{\underline{x}}(t) = \underline{f}(\underline{x}(t), \underline{p}), \ \underline{x}(t) \in R^n, \ \underline{f} \in R^n \tag{2.3}$$

with a set of parameters $\underline{p}$. The vector field $\underline{f}$ describes the time evolution of the states $\underline{x}$ and the n-dimensional space R^n spanned by the variables $x_1, \ldots, x_n$ is referred to as the *state space* or *phase space*. The graph of a particular solution $\underline{x}(t)$ in phase space is called a *trajectory* or *phase curve*. An *orbit* specifies the set of all points on a trajectory. Uniqueness of solutions to the system of equations (2.3) implies that no crossings of trajectories exist in phase space.

Certain systems are not described by a continuous set of differential equations but rather by a *map* or *first-order, autonomous, vector difference equation*

$$\underline{x}_{k+1} = \underline{g}(\underline{x}_k, \underline{p}) \tag{2.4}$$

Given a continuous system, a discrete map can be associated with it either analytically or experimentally in various ways, which will be discussed in Section 2.3. The discrete formulation is often more convenient since the analysis of the system can be performed without integration.

2.2. Basic Concepts of Chaotic Dynamics

Due to the critical dependence on the initial conditions, and due to the fact that, in general, experimental initial conditions are never known perfectly, chaotic systems are unpredictable. Indeed, the *prediction* trajectory emerging from an *experimental* initial condition and the *real* trajectory emerging from the *real* initial condition diverge exponentially in course of time, so that the error in the prediction (the distance between prediction and real trajectories) grows exponentially in time, until the system's real trajectory becomes completely different from the predicted one at long times.

Lyapunov exponents are a measure for the relative behaviour of initially close trajectories of a chaotic system. On the attractor, trajectories of a chaotic system show exponential divergence and convergence in different directions. The properly averaged exponents of this divergence or convergence are called *Lyapunov exponents*. A chaotic system must have at least one positive Lyapunov exponent. Chaotic systems with more than one positive Lyapunov exponent (divergence in at least two directions) are called *hyper-chaotic*.

The largest positive Lyapunov exponent provides a measure for the predictability horizon of a chaotic system. Consider two trajectories $\underline{x}_1(t)$, $\underline{x}_2(t)$ and let $\underline{x}_d(t) = \underline{x}_1(t)-\underline{x}_2(t)$ and $\underline{x}_d(0) = \underline{x}_1(0)-\underline{x}_2(0)$. Suppose that the initial conditions are close ($||\underline{x}_d(0)||$ small) and let λ^+ be the largest positive Lyapunov exponent. Then

$$||\underline{x}_d(t)|| \approx e^{\lambda^+ t} ||\underline{x}_d(0)|| \tag{2.5}$$

is an estimate of the divergence of the trajectories.

Depending on $\underline{f}$ (or $\underline{g}$) and initial values, trajectories will either go to infinity or stay in a bounded area forever. The set of initial conditions leading to the same asymptotic behaviour of the trajectory is called the *basin of attraction* [4]. The systems discussed in this thesis typically do not only have bounded solutions but are also *dissipative*, which means that on the average the phase space volume containing initial conditions is contracted under the dynamics. As a result, trajectories approach an attracting set A of measure zero that describes the asymptotic behaviour of the system and has the following properties [3]:

i. It is a compact set, invariant under the flow $\underline{f}$ or map $\underline{g}$, i.e. any trajectory $\underline{x}(t)$ or $\underline{x}_k$ starts in A stays in A for all time.
ii. A attracts an open set of initial conditions: there is an open set U containing A such that if $\underline{x}(0) \in U$, (or $\underline{x}_0 \in U$) then the distance from $\underline{x}(t)$ to A tends to zero as $t \to \infty$ (the distance between $\underline{x}_k$ and A tends to zero as $k \to \infty$). This means that A attracts all trajectories that start sufficiently close to it. The largest such U is called the basin of attraction of A.
iii. A is minimal (there is no proper subset of A that satisfies conditions i and ii.).

Regular (non-chaotic) attractors such as stable periodic orbits and stable equilibrium points characterise regular behaviour. Equilibrium point $\underline{x}^*$ of a continuous dynamic system is defined as,

$$\underline{f}(\underline{x}^*, \underline{p}) = 0 \tag{2.6}$$

and equilibrium point $\underline{x}^*$ of a discrete-time system is given by,

$$\underline{g}(\underline{x}^*, \underline{p}) = \underline{x}^* \tag{2.7}$$

On the other hand, dissipative chaotic systems have strange attractors as their attracting sets. Strange attractors usually have a fractal structure. Strange attractors can be

defined in different ways. Wiggins [4] defines a strange attractor A as an attractor, which has the properties (i) through (ii) and in addition the following property (iv).

iv. The dynamics in A are *sensitive dependent on initial conditions*: There is an $\varepsilon > 0$ such that, for any $\underline{x}(0) \in A$ and any neighbourhood N of $\underline{x}$, there exists a $\underline{y}(0) \in N$ and $t > 0$ such that $\| \underline{x}(t) - \underline{y}(t) \| > \varepsilon$.

Properties (i) - (iii) together with (iv) can be considered as conditions for defining a chaotic attractor. Devaney [5] adds a further characteristic property of chaotic attractors:

v. The periodic orbits of the dynamics are dense in A: Every ε *neighbourhood* of a point $\underline{x} \in A$ contains a point that belongs to a periodic orbit.

A chaotic system has many *Unstable Equilibrium Points* (UEPs) and usually infinitely many *Unstable Periodic Orbits* (UPOs) embedded into its strange attractor. Furthermore, all UEPs and UPOs in the strange attractor are of saddle-type.

The existence of saddle type UEPs and UPOs leads us to the concept of *ergodicity*. System dynamics in the chaotic attractor is called *ergodic*, which refers to the fact that during its temporal evolution the system visits a close neighbourhood of every point in the chaotic attractor. In other words, the behaviour of a dissipative chaotic system on its strange attractor can be considered as consisting of a single infinitely long trajectory approaching eventually any saddle-type UEP and UPO, but never staying at any of them because they are unstable.

In Figure 2.1 examples of regular and chaotic attractors are shown and Figure 2.2 shows several different UPO's of the Lorenz attractor in a two-dimensional projection.

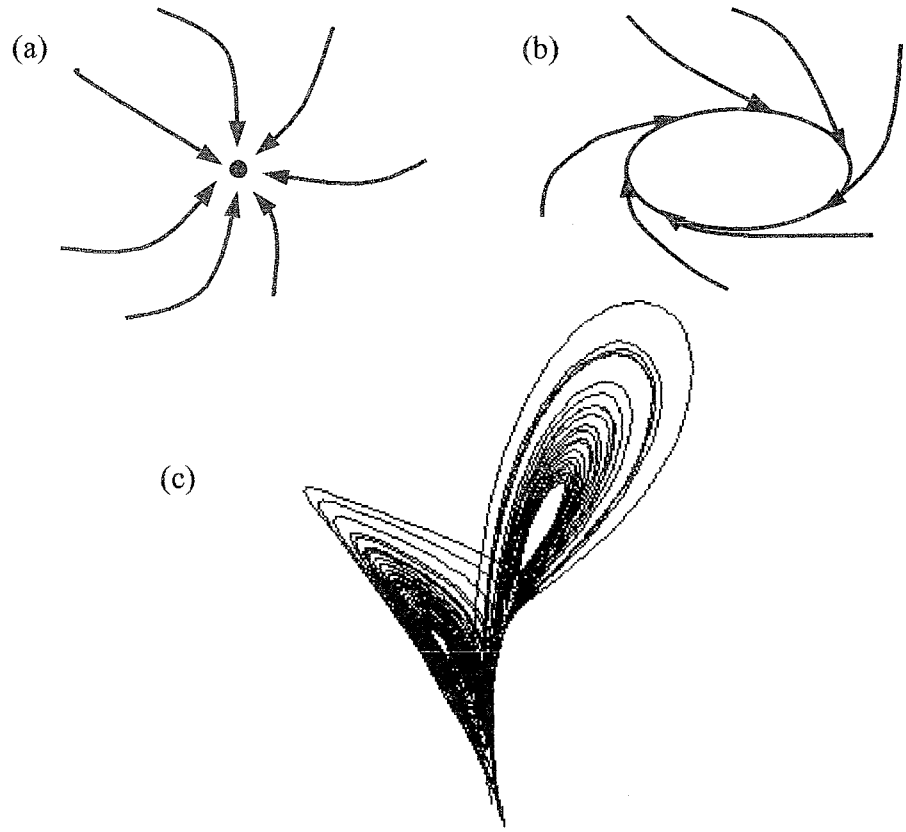

Figure 2.1. Examples of regular (a),(b) and strange (c) attractors

2.3. Discrete Representation of Continuous Dynamics and Determination of UPOs

Calculation of the equilibrium points is easy if the system dynamics is known but the determination of the periodic orbits is difficult, in general, and may be impossible. A method proposed by H. Poincaré [6] provides the possibility of introducing a discrete description for a continuous-time system in terms of the so-called *Poincaré map* illustrated in Figure 2.4. This mapping is important because it reduces the dimension of the system by one and often allows a good interpretation of the continuous dynamics in a discrete manner. The idea is to record the continuous trajectory whenever it pierces a certain surface-of-section Σ, which is a hyper-plane of dimension $(n-1)$, in a specified direction.

The Poincaré map $\underline{F}$ is a mapping from Σ to Σ showing a piercing of a system trajectory as a function of the previous piercing [4]. With $\underline{x}_k$ denoting the k^{th} piercing of Σ in the specified direction, the Poincaré map is defined by

$$\underline{x}_{k+1} = \underline{F}(\underline{x}_k) \tag{2.8}$$

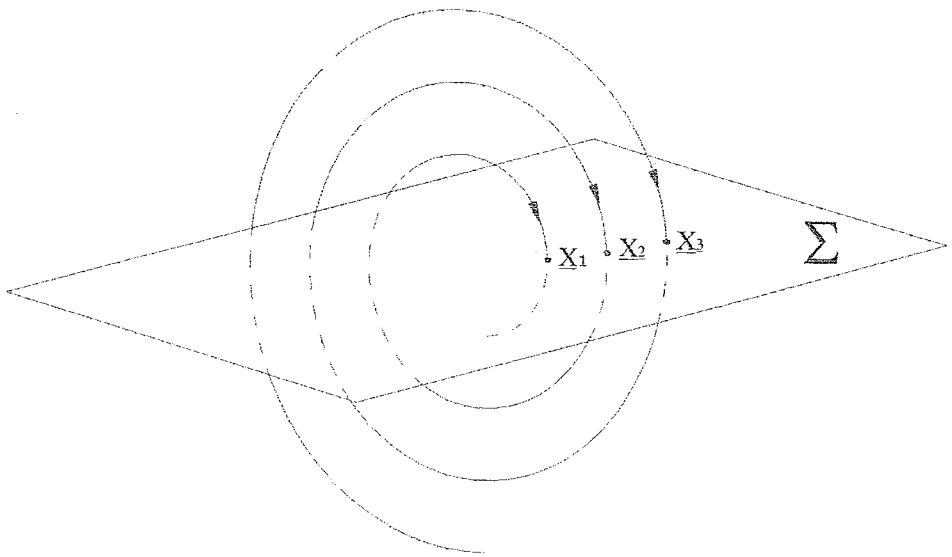

Figure 2.2. Illustration of a Poincaré map

It should be noted that the Poincaré map of an n-dimensional continuous-time system is (n-1) dimensional. The periodic points of the Poincaré map correspond to periodic orbits of the original continuous-time system. In particular, if the periodic orbit of the continuous-time system pierces Σ in a single loop, the piercing point will correspond to an equilibrium point (= period-1 point) of the Poincaré map. Hence, the detection and stabilisation of an unstable equilibrium point of a discrete-time system and that of an unstable periodic orbit of a continuous-time system using the Poincaré method are equivalent.

Methods to identify the location of UPOs can be divided into those, which assume experimental data, and others, which require an analytical description of the system dynamics. The simplest method to identify UPOs from experimental data relies on finding points of close return (*recurrent points*) in the Poincaré phase space [7].

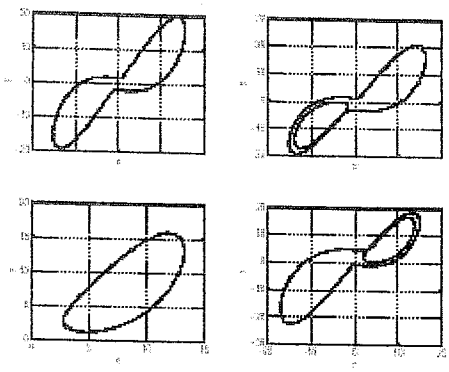

Figure 2.3. Different unstable periodic orbits of the Lorenz attractor

Assuming that dynamics are described by a map, a point $\underline{x}_m$ satisfying $||\underline{x}_{m+k} - \underline{x}_m|| < \varepsilon$ is called a (k, ε) recurrent point and corresponds to a periodic point of period k. A disadvantage of this method is that a large number of data points are necessary in order to accurately identify UPOs of large period. Furthermore, if ε is too large different UPOs might not be resolved. However, if ε is too small, not enough recurrent points might occur in reasonable time to allow the estimation of the UPO. In spite of these disadvantages, this *method of close returns* has been successfully applied to experimental data obtained from many chaotic systems for the detection of UPOs.

2.4. Lyapunov's Linearisation Method and Extraction of the Local Linear Model

In the late 19th century, the Russian mathematician Alexandr Mikhailovich Lyapunov introduced a general approach for studying the stability of non-linear systems. Lyapunov's approach includes two methods namely the linearisation method and the direct method. The linearisation method is concerned with the local stability of a non-linear system and describes mathematical relations between the non-linear system's local stability and stability properties of its local linear approximation. Lyapunov's linearisation method is considered as a justification of the usage of local linear approximation [8].

Equation (2.3) can be approximated near this equilibrium point by equation (2.9)

$$\underline{z}_{k+1} - \underline{z}^* = \underline{\underline{A}}\,(\underline{z}_k - \underline{z}^*) + \underline{b}(p - p_{nom}) \qquad (2.9)$$

where $\underline{\underline{A}}$ is an nxn Jacobian matrix of $\underline{f}$ and $\underline{b}$ is an n-dimensional column vector. $\underline{\underline{A}}$ and $\underline{b}$ are defined by the partial derivatives as,

$$\underline{\underline{A}}=\frac{\partial}{\partial \underline{z}}\,\underline{f}\,(\underline{z},p)\,\Big|_{z^*,\,p_{nom}}$$
$$\underline{b}=\frac{\partial}{\partial \underline{p}}\,\underline{f}\,(\underline{z},p)\,\Big|_{z^*,\,p_{nom}} \qquad (2.10)$$

and can be calculated by using a least-square error approach with experimental system data, assuming a polynomial behaviour.

2.5. Delay Coordinates Method

In many practical applications, as a result of the observation of just one system variable, system dynamics needs to be reconstructed. In this case, generally the *delay coordinates method* has to be employed.

If we denote this measurable variable by $y(t)$, choosing an appropriate delay time T and delay dimension d_e, a delay coordinate vector $\underline{s}(t)$ can be reconstructed as given in (2.11)

$$\underline{s}(t)=[y(t), y(t-T), y(t-2T), \ldots, y(t-d_eT)] \qquad (2.11)$$

Takens' Delay Map Embedding Theorem says that a delay map of dimension $2d + 1$ is an embedding of a compact manifold with dimension d.

If T and d_e are appropriately chosen [9, 10], there exists a diffeomorphism between the dynamics of the reconstructed new state vector and the real state vector [11]. As a result, reconstructed attractor is in one-to-one correspondence with the original attractor. The equilibrium points and periodic orbits in the real system have their counterparts in the delay coordinate system exhibiting the same stability properties.

It turns out, however, that it is not always necessary to have a one-to-one correspondence. Local stability properties around chosen UEPs and/or UPOs can be preserved with a delay map dimension $d_e < 2d + 1$ in many applications.

3. OGY CONTROL AND TARGETING

3.1. The Basic OGY Method

Chaos was regarded as undesirable due to its complexity and unpredictability. In engineering sciences, systems were designed such that chaotic dynamics would not occur. Pioneering work of Ott, Grebogi and Yorke [2], who proposed to control chaos by using the characteristics of chaos itself and showed that applying small perturbations to a parameter, could stabilise chaotic systems. This idea of chaos control is fundamentally different from the conventional engineering approach in control. The system stays in the chaotic regime during control but is stabilised at one of its unstable equilibrium modes.

In the OGY method, properly chosen small time-dependent perturbations, Δp, is applied to the system parameter p_0. After perturbation, local linear properties of the system dynamics around the desired target are slightly shifted. Since the OGY method is model independent, all necessary analytical knowledge can be extracted from experimental data.

Assuming that the dynamics can be described by a two-dimensional map,

$$\underline{x}_k = \underline{f}(\underline{x}_k, p_0 + \Delta p_k), \underline{x} \in R^2, p_0 \in R \tag{3.1}$$

the following formula will be used for calculation of the perturbation Δp_k.

$$\Delta p_k = \frac{\lambda_u f_u}{(\lambda_u - 1) f_u \cdot g} (\underline{x}_k - \underline{x}_f(p_0)) \tag{3.2}$$

In (3.2) $\underline{x}_f(p_0)$ denotes the location of the desired fixed point of the unperturbed system.

The *gain* g describes how $\underline{x}_f$ changes with p,

$$\underline{x}_f(p) \approx \underline{x}_f(p_0) + g \cdot \Delta p \tag{3.3}$$

such that

$$g \approx \frac{\underline{x}_f(p) - \underline{x}_f(p_0)}{\Delta p} \tag{3.4}$$

where λ_u denotes the unstable eigenvalue associated with the unstable eigenvector e_u of the Jacobian matrix of $\underline{f}$ evaluated at $\underline{x}_f(p_0)$, e_s represents the stable eigenvector, f_u denotes the adjoint unstable eigenvector defined as

$$< f_u \cdot e_u >= 1 \tag{3.5}$$

$$< f_u \cdot e_s >= 0 \tag{3.6}$$

The idea of the OGY method can be understood from Figure 3.1.

System state would approach the fixed point along the stable direction and move away from it along the unstable direction with nominal parameter value (Figure 3.1a). Because of perturbation, the local linear properties, stable and unstable manifolds, are slightly shifted such that the trajectory approaches the stable direction of the unperturbed system (Figure 3.1b). Consequently, the system state falls exactly on the stable manifold of the unperturbed system and the dynamics will approach the desired fixed point in the ideal case (Figure 3.1c). Since the OGY control scheme uses the local linear model, controller is only activated after the system state has reached a closed neighbourhood, N, of the desired target. Due to the ergodic behaviour of chaotic dynamics on the strange attractor, it is guaranteed that every trajectory eventually visits N.

The OGY control scheme has a local character, which results in an initial waiting time before control can be activated. This will be referred to as the *waiting time* τ. Letting $\mu(N)$ denote the rate at which random orbits fall into the region N, it follows that the average waiting time is $\langle \tau \rangle = 1/\mu(N)$ [12].

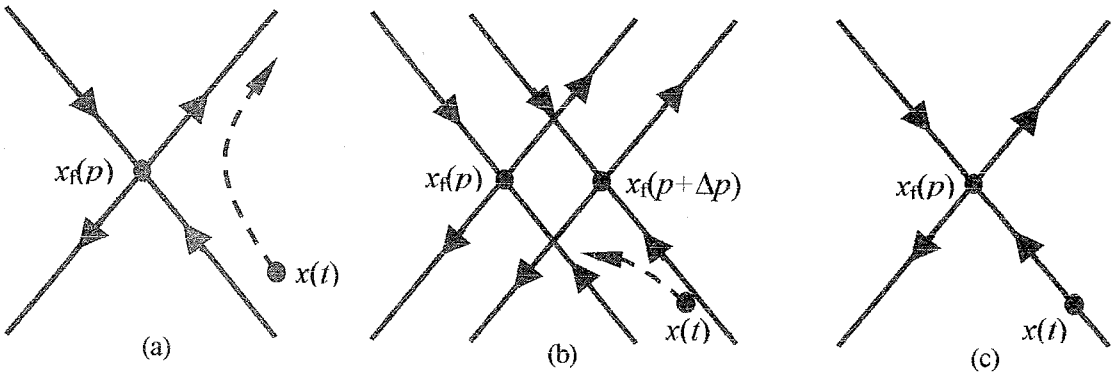

Figure 3.1 The idea of the OGY method

The size of the local control region, where OGY method's local linear model is valid, depends on the maximum allowed perturbation δ ($|\Delta p| < \delta$) and the local dynamics of f in this region. For one-dimensional maps one can show $\langle \tau_{ogy} \rangle \sim \delta^{-1}$ and for two-dimensional maps [12]

$$\langle \tau_{OGY} \rangle \sim \delta^{-\gamma}, \gamma = 1 + \frac{\ln|\lambda_u|}{2\ln|1/\lambda_s|} \tag{3.7}$$

Besides small control power expenditure, the main advantage of the OGY control scheme is that it is model independent. All necessary quantities describing the local dynamics close to the desired state can be approximated from experimental data. However, to compute the control formula, the desired state must be determined by analysing the experimental data. Any accessible system parameter can be used as the control parameter.

On the other hand, given an accurate control formula, small noise can destabilise the chaotic orbit. In real applications, in case of existence of noise, the determination of the desired UPO and in particular the estimation of the linearised dynamics will become less accurate. Thus the influence of noise is twofold: it can kick the dynamics out of the controllable region and it can affect the accuracy of the control formula.

To apply the OGY method, the location of the fixed point has to be known in advance. In addition to that, in the case of non-stationarity this location will shift and the OGY control formula will become inaccurate. Besides its drawbacks, the OGY method remains one of the most popular chaos control method and has been successfully applied to many experimental systems.

Many extensions and improvements of the OGY method have been proposed. In [13] the multi-parameter control case is investigated and the application of the OGY control method to delay coordinates is discussed in [14, 15]. The extension concerning high-dimensional chaotic systems is discussed in [16, 17, 18].

The OGY method has been revised and extended to higher dimensions by allowing a more general choice of the feedback matrix by Romeiras *et al* [16]. In this extension involving the *pole placement technique,* the OGY method is formulated as a pole placement problem and is solved by placing the regulator poles at desired locations.

In this extension, first, the dependence of the system dynamics on the parameter change has to be determined. For this purpose, the parameter change is assumed to be a linear function of the variable $\underline{z}_n$ of the form given in (3.8),

$$(p-p_{nom})= -\underline{h}^T (\underline{z}_k-\underline{z}^*) \tag{3.8}$$

where h is an n-dimensional row vector. Substituting (3.8) into (2.11) yields

$$\underline{z}_{k+1}-\underline{z}^*= (\underline{\underline{A}} -\underline{b}\, \underline{h}^T) (\underline{z}_k-\underline{z}^*) \tag{3.9}$$

If the eigenvalues of $(\underline{\underline{A}} -\underline{b}\, \underline{h}^T)$ have an absolute value smaller than unity, $(\underline{\underline{A}} -\underline{b}\, \underline{h}^T)$ is asymptotically stable, and $(\underline{z}_{k+1}-\underline{z}^*)$ goes to zero as time goes to infinity. This means that the equilibrium point will be stable.

The problem is to determine $\underline{h}^T$ such that $(\underline{\underline{A}} - \underline{b}\,\underline{h}^T)$ is stable. The solution is referred to as the Pole Placement Technique and the desired locations of the poles of $(\underline{\underline{A}} - \underline{b}\,\underline{h}^T)$ are accomplished by choosing the proper $\underline{h}^T$.

A further popular variant of the OGY method is the *occasional proportional feedback* (OPF) method [19]. This method and its variants [20, 21] feed deviations of the chaotic variable from an a priori fixed point back into the system as parameter perturbations whenever the system variable enters a specified window.

A prediction-correction scheme based on the OGY method has been suggested by Schwartz *et al.* [22]. Bielawski *et al.* [23] have modified the control formula directly to use the difference between consecutive iterates of the map instead of the difference between each iterate and the fixed point as in the OGY formula. In a later work Bielawski *et al.* [24] have extended the discrete- time version to continuous-time parameter perturbations.

3.2. Targeting

In the literature, the first attempt to reduce the transient time was done by Shinbrot *et al* [25] who have theoretically and numerically demonstrated that trajectories on a chaotic attractor can be steered to a desired target by small perturbations of the system parameter. Then, they have implemented their method for a system describable by a one-dimensional map [26], and have applied it to real system [27]. In [26] it is stated that this method is applicable only to chaotic systems, whose strange attractor have a Poincaré section with a fractal dimension close to one. Nevertheless, the method has been extended to higher dimensions (four-dimensional double rotor map with two positive Lyapunov exponents) and been refined via tree-type hierarchy in [28].

Barreto *et al* used the same method to steer the trajectories of the double rotor to any of the unstable periodic orbits chosen as targets, and then it has been shown that it is possible to switch the system between those chosen unstable periodic orbits [29]. In [30],

targeting is realised by creating periodic orbits via P-chain perturbations without changing the topology of the system such that the system repeats itself at each M^{th} iteration.

In [31], Paskota *et al* have employed optimal control techniques to bring the system states to a desired state under some constraints [32]. Another goal of Paskota *et al* when developing this method was to improve the performance of the system against random noise [33]. However, their method is still initial condition dependent, i.e., it is not global. In [34], in order to eliminate this initial condition dependence, a mixed strategy is developed making the controller more global. Paskota and Lee have also employed the optimal control techniques for targeting the systems to a moving target [35]. However, the methods proposed in [31-34] necessitate the exact equations of system dynamics. The method proposed in [30] is implemented in [36], where the global system model is obtained via wavelet networks. Baptista used ε-bounded orbit correction perturbations for targeting purposes in a kicked double rotor [37].

Another technique for chaos control based on reinforcement learning combined with a vector quantisation of the state space, is introduced by Gadaleta *et al* [38]. Since this method does not require an analytical description of the underlying dynamics, it can handle both perturbations of a control parameter as well as perturbations in the form of proportional pulses applied to a state variable.

Extended Control Regions (ECR) method, which will be explained in further detail in the next section and does not require any analytical information about the system dynamics, has been developed and implemented by the use of neural networks by Iplikci and Denizhan [39, 40].

4. ANALYTICALLY MODELLED CLUSTERS METHOD

The idea of identifying different regions of the phase space, starting from which the system can be steered towards the chosen target within some steps using allowable parameter variations, has been developed and improved by Iplikci and Denizhan [39, 40, 41]. This method and its improved versions, namely Extended Control Regions (ECR) Methods, are based on modelling of these control regions and the corresponding control policies by the aid of Radial Basis Function (RBF) based Neural Networks.

The method proposed in this thesis referred to as Analytically Modelled Clusters (AMC) Method is an application of the Clustered-ECR-II approach without using neural networks. Rather than that a simple analytical description is used as a modelling tool. The employment of such an analytical description requires some modifications in the data gathering and control phases. For this purpose two different data gathering strategies and the related control strategies have been developed, which are referred to as AMC-I and AMC-II.

4.1. Introduction

The waiting time until the system enters the close neighbourhood of the target (the OGY region) may be quite long depending on the initial conditions and the size of the strange attractor. Therefore, before the application of OGY control most chaotic systems require targeting, i.e. a way of steering the system from any initial point towards the OGY region.

Since targeting requires global information about the strange attractor, local approximations are no longer sufficient. The proposed methods, which will be referred to as AMC-I and AMC-II, do not use a complete model of the strange attractor but cover a sufficiently large part of the attractor by hyper-ellipsoids for satisfactory targeting.

Before going into the details of AMC methods, it will be helpful to explain briefly the basic idea behind the ECR approach.

4.2. Extended Control Regions Method (ECR)

The approach used in the ECR method is to extend the phase space regions where the controller is activated. These regions and the corresponding control actions are modelled by the aid of Radial Basis Function (RBF) based neural networks. After these regions and corresponding control policies have been modelled, it is supposed that the system can be steered step by step from one of these regions to the OGY region and the chosen target can be stabilised.

In the ECR-I, firstly, the chaotic system is run while perturbing the control parameter randomly within its allowable range to gather experimental system data. Analysing experimental data obtained from this randomly perturbed system, data points, which fall into the OGY region in a few steps, are used to identify control regions of the phase space.

In the first version of the Extended Control Regions method, ECR-I, a single neural network is used for both targeting and local control purposes. After this single neural network is trained by experimental data, it is used to obtain the necessary control parameter perturbation for steering the system state to the chosen target. In this version, information about the region of the current system state is hidden in the neural network and cannot be observable. If the neural network gives a parameter value out of the allowable range, the parameter value is set to its nominal value and wait for the next iteration.

As a result of using a single neural network, modelling errors in ECR-I are highly probable especially between different control regions. In addition to that, the region of the current state is not available externally. In spite of such disadvantages, ECR-I exhibited an acceptable improvement in terms of the average waiting time. While defining waiting time as the time necessary to steer the system to the OGY region starting from an initial condition, average waiting time can be defined as the average of the waiting times over many randomly chosen initial conditions.

In the second version, ECR-II, the targeting performance has been improved by dedicating a separate neural network to each control region. After determining the regions of the phase space from experimental data, each neural network is trained using data from

the corresponding control region. In ECR-II also a heuristic method has been introduced for the determination of the region of the current state. Current state is fed to the trained neural networks in a sequential manner starting from the lowest index and when a neural network gives a control parameter value within the allowable range, it is assumed that the current system state belongs to the region associated with that neural network. Consequently, this neural network is activated for targeting. Although this improved version shows a better performance in most chaotic systems, there still exist some modelling errors due to the fact that data belonging to higher-level control regions are more scattered.

In the last version of the ECR, Clustered-ECR-II, the modelling performance is improved by subdividing each control region into sub-regions, where the experimental data are clustered. In this version a separate neural network is assigned to each sub-cluster. This improvement reduces the modelling errors in ECR-II in inter-cluster regions on cost of increasing the number of neural networks employed.

Besides this modification, clusters are represented analytically by their means and normalised covariance matrices. Using this analytical description, the region of current system state can be determined analytically. The same approach is adopted in the proposed method and will be explained in further detail in the following sections. Although the number of neural networks used in Clustered-ECR-II is larger than in ECR-II, most of the performance criteria such as memory usage and total training time of neural networks are improved. These performance criteria and the comparison of different versions of ECR methods are summarised in Table 5.1 and also their performances are compared to the proposed method's results for the same chaotic systems.

Targeting and control approach of ECR methods is illustrated in Figure 4.1.

4.3. Main Idea of the Analytically Modelled Clusters (AMC) Method

Having observed the improvement of the targeting performance by the introduction of sub-clusters, the next question was whether a simpler model of the system dynamics

within these clusters might be possible. This question finally has given rise to the proposed targeting method, namely the Analytically Modelled Clusters (AMC) method.

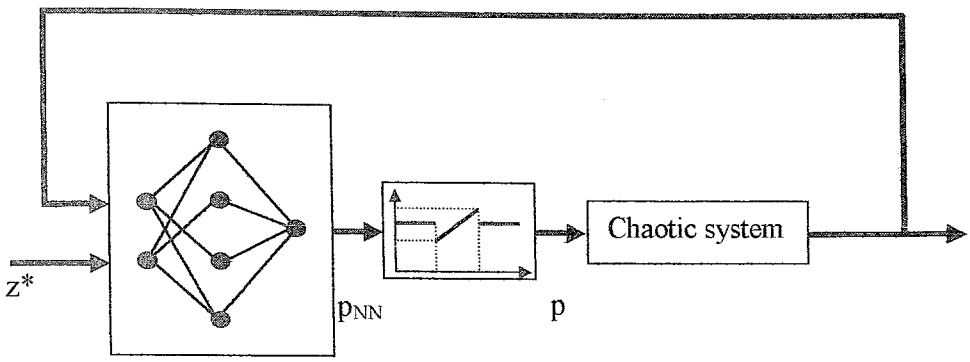

Figure 4.1. Control loop for targeting and control via neural networks

The Analytically Modelled Clusters (AMC) method is a targeting method applicable to chaotic systems with unknown dynamics. Although theoretically applicable to systems with several control parameters, the AMC approach is more efficient for single control parameter applications.

AMC adopts a similar approach like in Clustered-ECR-II, namely system data belonging to different regions are gathered and subsequently grouped into sub-clusters. Likewise, the sub-clusters are represented in terms of their means and normalised covariance matrices. The basic innovation in AMC is the elimination of neural networks for modelling purposes providing a considerable simplification in the modeller and the controller.

In order to be able to model the system dynamics without the aid of neural networks the dynamics has to be simplified imposing additional constraints. In AMC this is achieved by replacing the continuous allowable range of the control parameter as used in the ECR methods (Π_1 as defined in equation (4.3)) by 3 discrete allowable parameter values, namely minimum (p_{min}), nominal (p_{nom}) and maximum (p_{max}) values.

In this work two different versions of the AMC approach have been developed.

The basic idea behind the AMC Method is to identify different regions $\{S_i^q$; i = 0, 1, ..., K; q = min, nom, max$\}$ for AMC-I and $\{T_i^q$; i = 0, 1, ..., K; q = min, nom, max$\}$ for AC-II of the phase space, where the controller will be activated. Hence, the control region of the controller is extended from S_0 (as used in the OGY control) to the union of S_0 and all S_i^q's (i = 1, ..., K; q = min, nom, max) in AMC-I and union of T_0 and all T_i^q's (i = 1, ..., K; q = min, nom, max) in AMC-II.

AMC Methods have four different phases,

i. Data gathering with appropriate control parameter values
ii. Analysis of data sets and determination of the control regions
iii. Determination of analytical descriptions of the sub-clusters of the control regions
iv. Control of the chaotic system using the analytical descriptions obtained

While the first three phases, (off-line phase) are different in AMC-I and AMC-II, the last phase, (on-line or control phase) is entirely the same in both versions.

As in the OGY control, it is assumed that *a priori* knowledge about system dynamics is not available, and that only system parameter(s) can be used for control purposes. The AMC methods are also applicable when delay coordinates are employed. The AMC method will be presented for n-dimensional discrete-time chaotic systems with a single control parameter only. This model covers both continuous-time systems with an unstable periodic orbit as the target (via Poincaré section method) and discrete-time systems with an unstable equilibrium point as a target. Such a system is represented by the following equation (4.1).

$$\underline{z}_{k+1} = G(\underline{z}_k, p) \tag{4.1}$$

where $\underline{z}$ is the nx1 state vector, and p is the rx1 control parameter vector.

Assume that this system has an equilibrium point at $\underline{z}^*$ described by,

$$\underline{z}^* = G(\underline{z}^*, p_{nom}) \tag{4.2}$$

where p_{nom} is the rx1 control parameter vector..

The control variable (parameter), which will be used for control purposes in the OGY region, can be changed within an allowable range as given in (4.3).

$$\Pi_1 = \{p : p_{nom} - \delta p_{max} < p < p_{nom} + \delta p_{max}\} \tag{4.3}$$

where δp_{max} is the maximum allowable parameter change for the control parameter.

Outside the OGY region, the control variable (parameter) can be chosen in a discrete manner from the set given in (4.4)

$$\Pi_q = \{p_q\} \text{ where } q = \text{min, nom, max.} \tag{4.4}$$

where

$$p_{min} = p_{nom} - \delta p_{max} \text{ and } p_{max} = p_{nom} + \delta p_{max} \tag{4.5}$$

When explaining the procedures for AMC-I and AMC-II it will be assumed that the necessary pre-processing (Poincaré section for continuous time systems or delay coordinates construction for systems where a single output can be observed) to represent the system in the form of (4.1) have been accomplished and $\underline{z}^*$ has been chosen as the target.

In order to explain the determination of these control regions, some definitions, have to be introduced.

Definition 4.1: $\underline{z}_k \in S_0$ if it satisfies (4.6)

$$\|\underline{z}_k - \underline{z}^*\| < \delta, \quad \text{and} \quad \|G(\underline{z}_k, p) - \underline{z}^*\| < \delta \quad \text{with } p \in \Pi_1 \tag{4.6}$$

In other words, starting from any $\underline{z}_k \in S_0$ the system can be kept within the δ neighbourhood of $\underline{z}^*$ at the next step using a $p \in \Pi_1$.

Definition 4.2: $\underline{z}_k \in S_1^q$ if it satisfies (4.7)

$$G(\underline{z}_k, p_q) \in S_0 \tag{4.7}$$

Definition 4.3: $\underline{z}_k \in S_i^q$ if it satisfies (4.8).

$$G(\underline{z}_k, p_q) \in S_{i-1}^q,\ i = 2,\ldots,K\ ;\ p_q \in \Pi_q \tag{4.8}$$

In other words, S_i^q is the set of states starting from which the system can be steered to S_{i-1}^q in one step using corresponding parameter value p_q.

In what follows, new regions T_i^q's in addition to the S_i^q regions in AMC-I will be defined for AMC-II.

Definition 4.4: $\underline{z}_k \in T_i^q$ if it satisfies (4.9).

$$G(\underline{z}_k, p_q) \in T_{i-1}^j,\ i = 2,\ldots,K\ ;\ j = \min, \text{nom}, \max\ ;\ p_q \in \Pi_q \tag{4.9}$$

The region T_i^q is the set of states, starting from which the system can be steered to one of three lower lever control region T_{i-1}^j in one step by applying a control parameter value p_q.

Before going into the detail of the application procedures of the AMC methods, it can be useful to give some information about data clustering and explain the clustering algorithm used in both Clustered-ECR-II and the AMC Methods.

4.4. Data Clustering

Data analysis is a very important part of computational applications. Data analysis procedures can be classified as either exploratory or confirmatory, based on the availability of appropriate models for the data source. The key element in both types of procedures is the grouping, or classification of measurements based on either goodness-of-fit to a model, or natural groupings (clustering).

Cluster analysis is the organisation of a collection of patterns (usually represented as a vector of measurements) into clusters based on similarity. Intuitively, patterns within a valid cluster are more similar to each other than they are to a pattern belonging to a different cluster [42].

It is important to understand the difference between clustering (unsupervised classification) and discriminant analysis (supervised classification). In supervised classification, a collection of *labelled* (pre-classified) patterns is provided; the problem is to label a newly encountered, yet unlabeled, pattern. Typically, the given labelled (*training*) patterns are used to learn the descriptions of classes, which in turn are used to label a new pattern. In the case of clustering, the problem is to group a given collection of unlabeled patterns into meaningful clusters. In a sense, labels are associated with clusters also, but these category labels are obtained from the data.

4.5. The Clustering Algorithm Used in the AMC Methods

It should be noted that theoretically an identified control region S_i^q (or T_i^q) extracted from experimental data does not need to be simply connected or connected; furthermore, successive regions can even be interlaced. As a matter of fact, the real regions have most of the time a fractal geometry.

On the other hand, any description of S_i^q's (or T_i^q's) will usually fail to capture their fractal nature because they are based on finite data. Consequently, the analytical description of S_i^q's (or T_i^q's) will only be approximations of the real S_i^q's (or T_i^q's).

It is quite reasonable to expect that data belonging to higher-level control regions are more scattered than those of the lower-level control regions. Theoretically it may seem paradoxical to try to cluster such data originating from a fractal pattern. However, it should be noted that in practice only finite data are available from such a fractal pattern. Consequently, the data fail to capture the fractal geometry and therefore the representation of data clusters as Euclidean objects is justified. Clustering provides more accurate analytical descriptions for these regions, especially for the higher-levels, and hence reduces the insufficient identification of control regions. Another point that has to be mentioned is the fact that, although the clustering algorithm used in ECR and AMC methods is very simple, it improves the controlling performance enormously.

The clustering algorithm used for determining any cluster C_{ij}^{q} of a control region S_i^q (or T_i^q) can be explained as follows:

An arbitrary data point in a control region, T_i^q, is taken as a centre of a hyper-sphere with a radius r and all data points that lie in that hyper-sphere are labelled with the same index, which is equal to 1 (j = 1) at the beginning. Next, another data point in same control region is taken as a new centre of the hyper-sphere. At this step, there are two possible situations:

i. If this new data point has a label, the clustering continues with another point.
ii. If not, a hyper-sphere is considered, the centre of which is the new data point. In this hyper-sphere a labelled datum is searched for.
    - If a labelled datum can be found in that hyper-sphere, all new data points in that hyper-sphere are labelled with the same index as the pre-labelled data point.
    - If not, this new data point is labelled by an incremented index number, j = j + 1.
iii. The clustering algorithm is terminated when all data points in the control region under consideration are exhausted.

In this algorithm, the radius of the hyper-sphere, r is obtained from the region data by visual analysis of the histogram of inter-data distances as the first minimum of the histogram. The clustering algorithm explained above is illustrated in Figure 4.2.

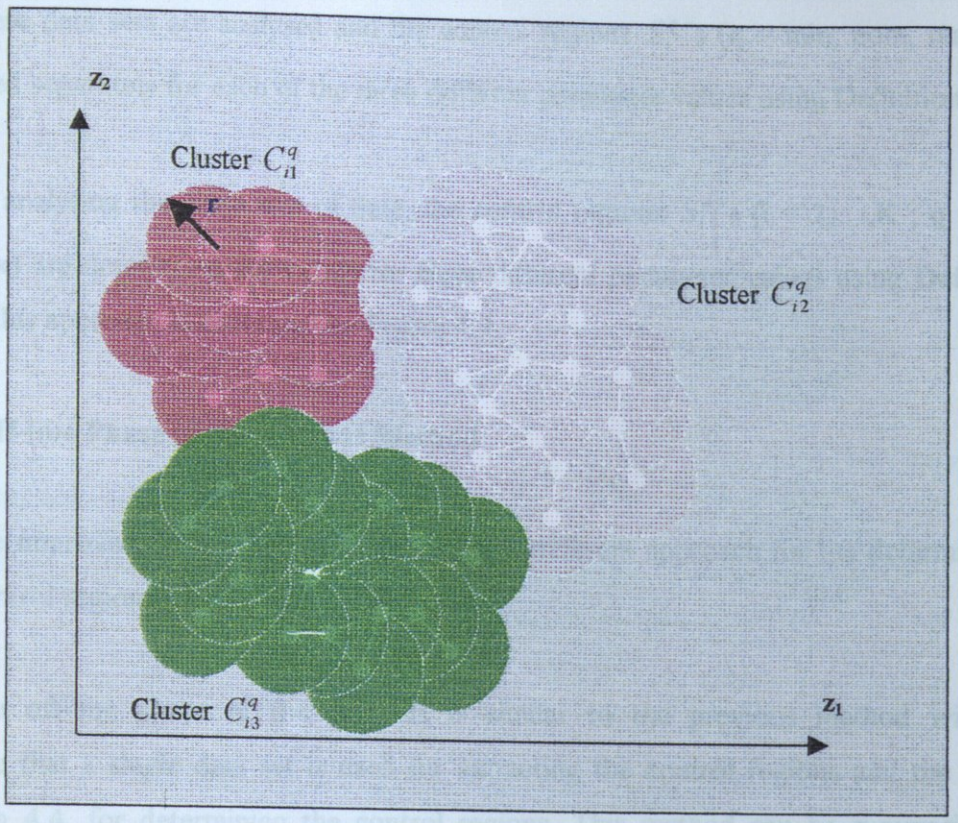

Figure 4.2. Illustration of the clustering algorithm used in AMC Methods

4.6 Application of the AMC Method

Since the off-line phases for different versions of the AMC method are different, they will be explained in subsections 4.6.1 and 4.6.2 consequently and in the subsection 4.6.3 control phase of this method will be discussed.

4.6.1. Off-line Phase of the AMC-I Method

Application of the procedure associated with the off-line phase of the AMC-I method can be described as follows:

The system is run three times with three different control parameter values, which are p_{min}, p_{nom} and p_{max}, until some predetermined termination criterion is satisfied. Three data sets containing the successive state pairs ($\underline{z}_k$, $\underline{z}_{k+1}$) are obtained from each a run.

These data sets are analysed and the control regions S_i^q's (q = min, nom, max) are determined separately for each of the three different parameter values using Definition 4.2.

By analysing the same sets of data, the control regions S_i^q's (i = 2,...,K ; q = min, nom, max) are determined separately for three different parameter values using Definition 4.3 and this approach is illustrated by Figure 4.3.

4.6.2. Off-line Phase of the AMC-II Method

The improvement in AMC-II is the use of a different approach for the determination of the control regions.

The off-line phase of the AMC-II is similar to the previous method with the difference that a single data set is used for extracting the control regions and the use of Definition 4.4. for determining the control regions. This method can be summarised as follows:

The system is run while changing the control parameter randomly in a discrete manner between the three possible values (p_{min}, p_{nom} and p_{max}) until some predetermined termination criterion is satisfied. The data set obtained from such a run contains the successive state pairs ($\underline{z}_k$, $\underline{z}_{k+1}$) and the corresponding parameter values (p_q 's where q = min, nom, max).

The procedure associated with the determination of the first level control regions (T_1^q's) of the AMC-II method is same as in the first method.

After the extraction of data belonging to T_0 and T_1^q's according to Definition 4.1 and Definition 4.2 ($T_0 = S_0$), the data belonging to T_i^q (for i = 2,...,K) are extracted according to Definition 4.4 as opposed to AMC-I.

The idea of this second method is illustrated in Figure 4.7.

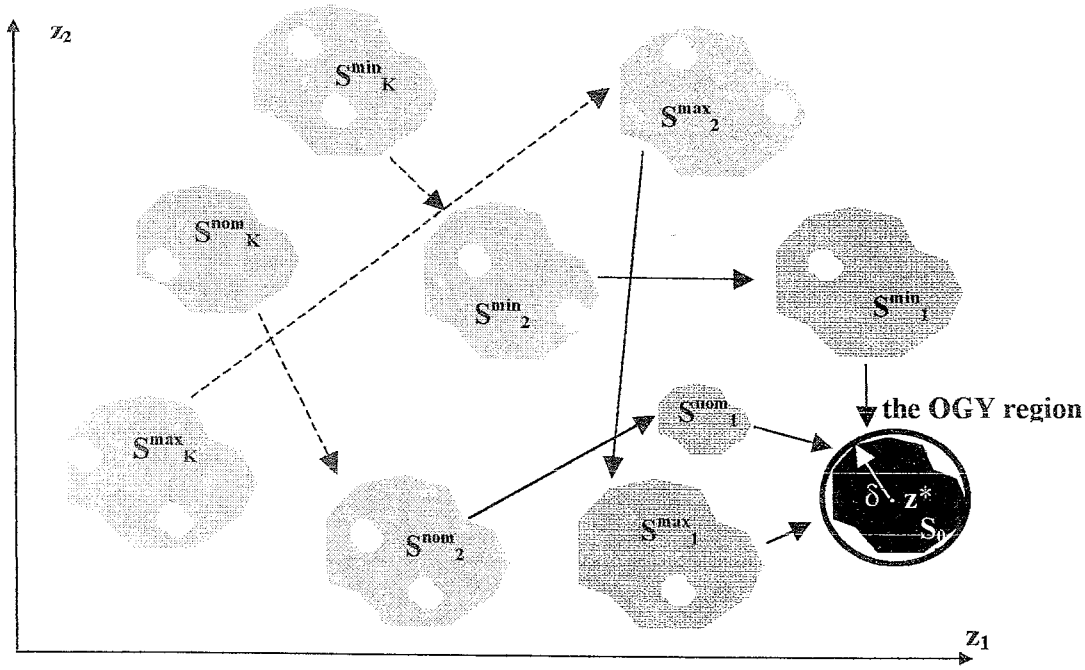

Figure 4.3 The idea of AMC-I Method

Before determining the analytical descriptions of the control regions, experimental data belonging to these regions need to be clustered for higher modelling accuracy. Although these data sets have a fractal nature, in order to cope with highly scattered finite number of data points belonging to the control regions, it is indispensable to pre-process data by a clustering algorithm like the one explained in the subsection 4.4.

After the clusters, C_{ij}^{q} belonging to the regions S_i^q for AMC-I and T_i^q for AMC-II have been obtained, the "Normalised Covariance Matrix" of the cluster C_{ij}^{q} denoted by $\underline{\underline{N}}_{ij}^{q}$ and the mean of cluster C_{ij}^{q} denoted by $\underline{\mu}_{ij}^{q}$ are calculated and the regions are analytically described as hyper-ellipsoids in terms of $\underline{\mu}_{ij}^{q}$'s and $\underline{\underline{N}}_{ij}^{q}$'s.

Off-line phases of the two different versions of AMC methods are illustrated in Figure 4.4 and data point belonging to first level control regions for Logistic Map for different versions of AMC Methods are given in the Figure 4.6.

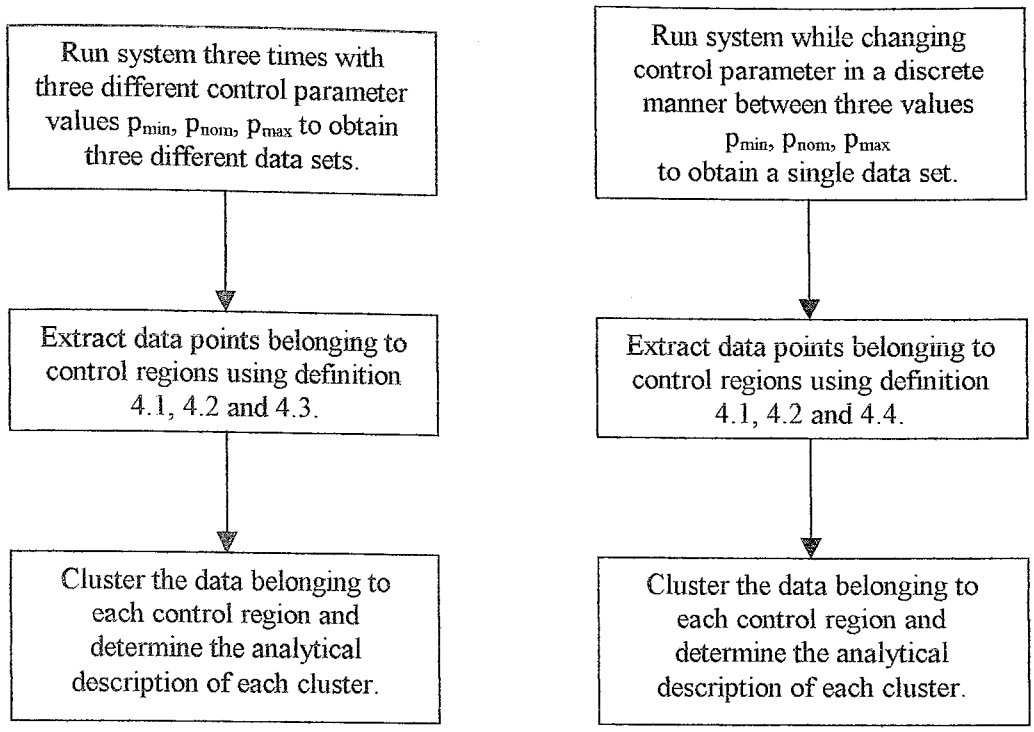

Figure 4.4. Flow-charts describing off-line phases of (a) AMC-I and (b) AMC-II

Data points belonging to some clustered control regions determined for different chaotic systems are illustrated ((a) T_2^{nom} for Lorenz System (Poincaré section) with r = 0.3, (b) T_1^{min} for Logistic Map with r = 0.2, (c) T_3^{max} for Hénon Map with r = 0.2, (d) T_4^{nom} for Hénon Map with r = 0.2) in Figure 4.5.

4.6.3. Control Phase of the AMC Methods

Analytical representation obtained after the clustering process allows the determination of the current state location in an analytical manner as follows:

For the current state $\underline{z}_k$, "Normalised Mahalanobis Distances" (NMD) from all C_{ij}^q's are calculated using the following equation.

$$(NMD_{ij}^q)^2 = (\underline{z}_k - \underline{\mu}_{ij}^q)^T \underline{\underline{N}}_{ij}^q (\underline{z}_k - \underline{\mu}_{ij}^q) \qquad (4.10)$$

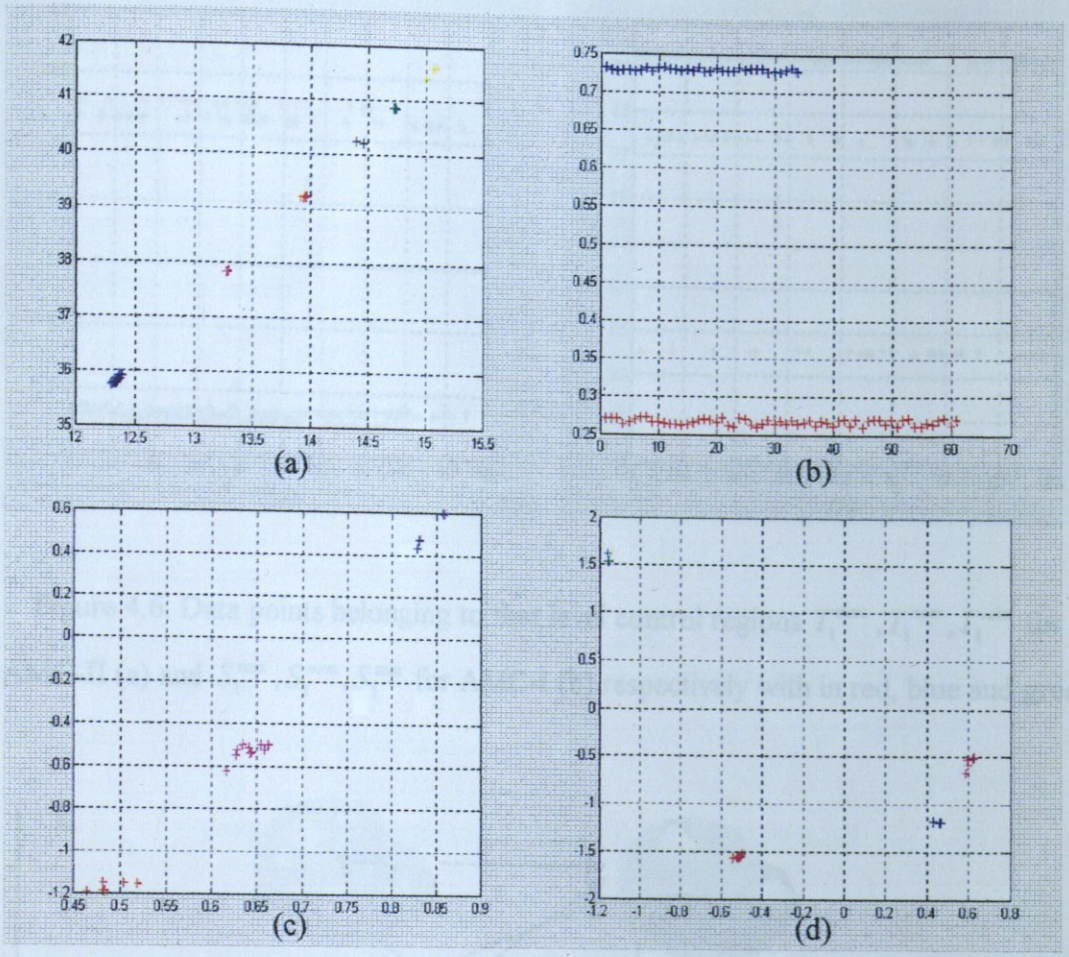

Figure 4.5. Some clustered control regions determined for different chaotic systems

The cluster C_{ij}^{q}, which has the minimum Normalised Mahalanobis Distance NMD_{ij}^{q} from the current state, is regarded as the region of the current state and the corresponding control parameter $p(k) = p_q$ applied to the system for targeting. If all distance measurements obtained by using equation (4.10) from current state are larger than unity, the current state is assumed to be in none of the control regions and no targeting action is taken which means that $p(k)$ is set to the nominal control parameter value p_{nom}. After this perturbation, controller waits until the next value of the new state of the system is obtained.

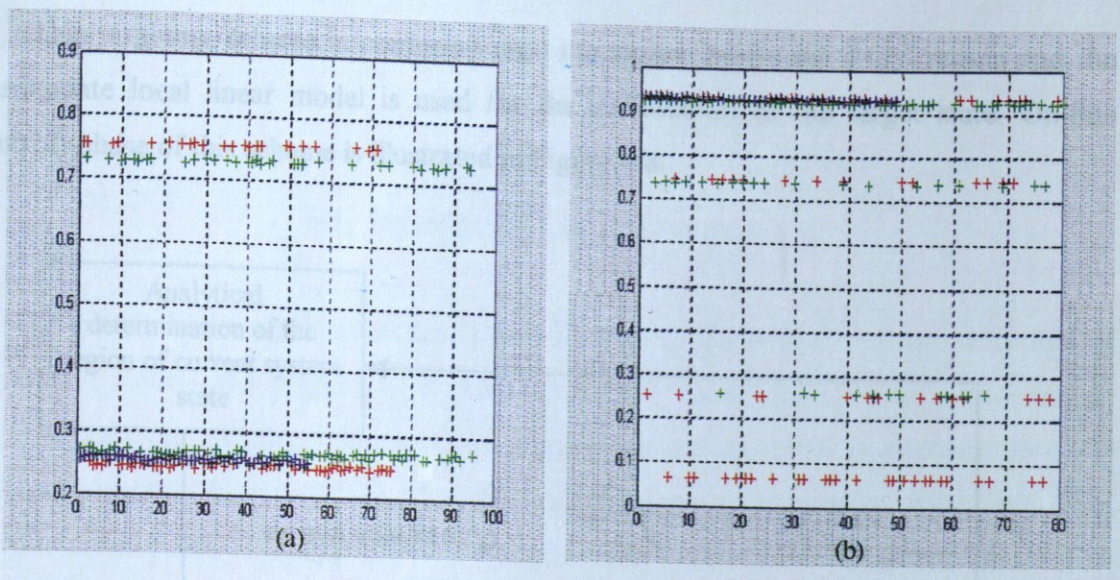

Figure 4.6. Data points belonging to first level control regions $T_1^{\max}, T_1^{nom}, T_1^{\min}$ for AMC-II (a) and $S_1^{\max}, S_1^{nom}, S_1^{\min}$ for AMC-I (b) respectively with in red, blue and green

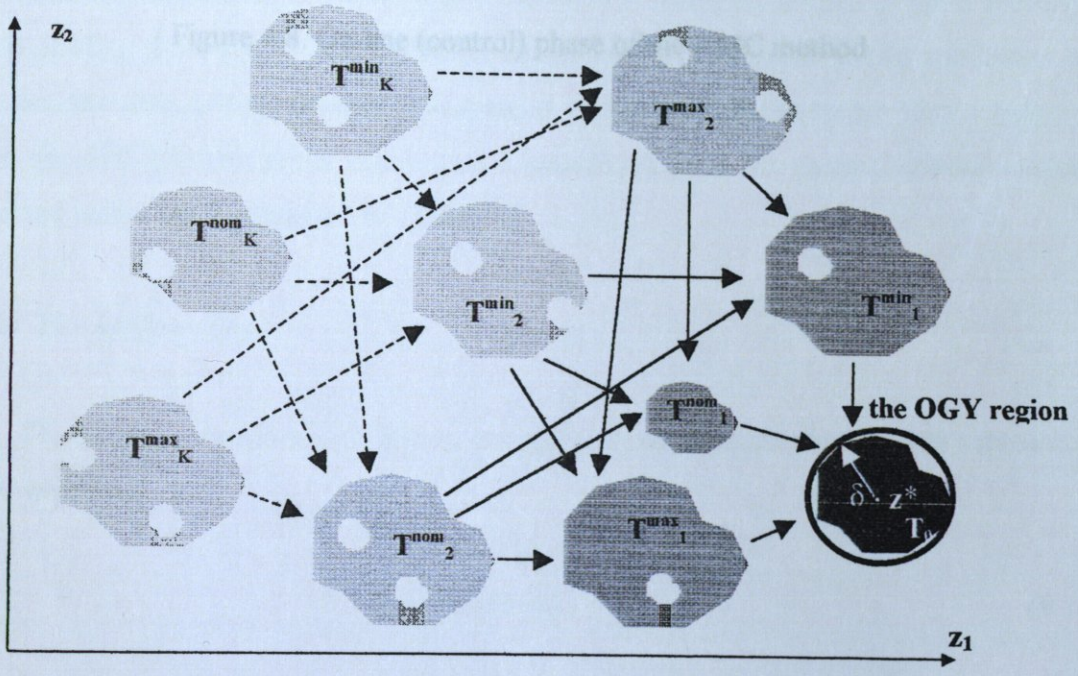

Figure 4.7. The idea of the AMC-II method

This targeting scheme is continued until the system enters the OGY region and the approximate local linear model is used for the stabilisation of the target state. On-line (control) phase of this scheme is illustrated in Figure 4.8.

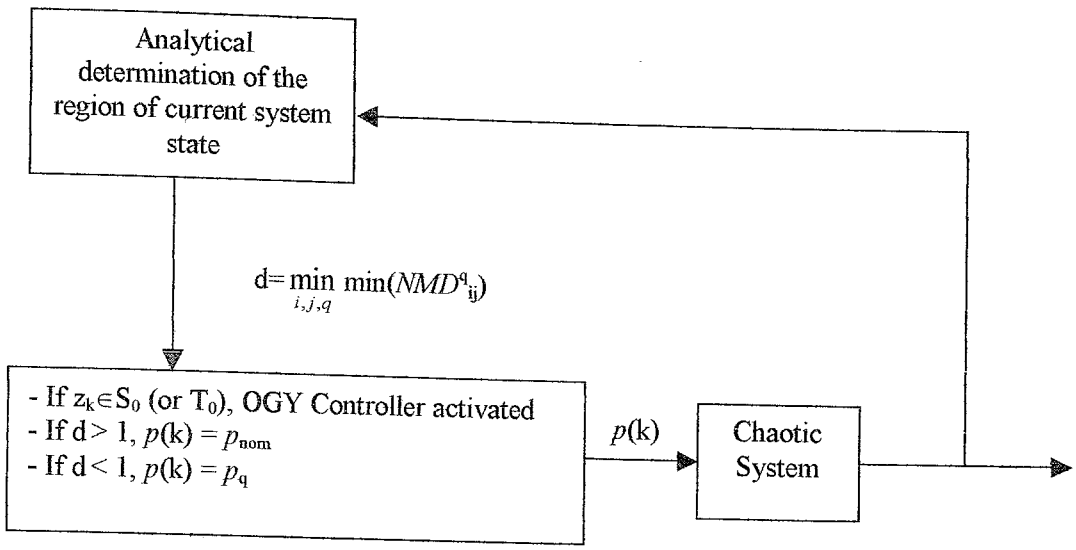

Figure 4.8. On-line (control) phase of the AMC method

5. SIMULATION RESULTS

5.1. Investigated Chaotic Systems

In this study, in order to compare the performance of the AMC method with that of the ECR methods, the original ECR simulations [43] have been used as a benchmark. These include various chaotic systems both under noiseless and noisy conditions. In order to determine the robustness of the AMC methods with respect to measurement noise, some random noise proportional to the root mean square value of the measured data (state measurement) is added. The maximum tolerable (i.e. allowing the stabilisation of the target) percentage measurement error is determined separately for each chaotic system and each control method (OGY, AMC-I and AMC-II). Furthermore, the average waiting time is determined for each system and each method under noisy conditions. The average waiting time is calculated as the average of the time it takes the system to enter the OGY region starting from many different initial conditions (500 different initial conditions for both discrete-time and continuous-time systems except for Double Rotor Map which was tested for 200 different initial conditions). Results obtained for various chaotic systems presented below are summarised in Table 5.1.

5.1.1. The Logistic Map

The Logistic map is a well known one-dimensional discrete-time system represented by the equation,

$$x_{n+1} = p x_n(1-x_n) \tag{4.11}$$

where p is the control parameter. The Logistic map exhibits chaotic behaviour for $p_{nom} = 3.9$, and for that value it has an unstable equilibrium point at $x^* = 0.7435$. In simulations, maximum allowed parameter change is taken as $\delta p_{max} = 0.10$ and the radius of local control region as $\delta = 0.01$. The root mean square of the measured state is found as $x_{rms}^{Logistic} = 0.6608$.

5.1.2. The Hénon Map

The Hénon map is a two-dimensional discrete-time non-linear system, which is represented by the relations,

$$\begin{aligned} x_{n+1} &= p + 0.3y_n - x_n^2 \\ y_{n+1} &= x_n \end{aligned} \tag{4.12}$$

where p is the control parameter of the map. The Hénon map exhibits a chaotic behaviour at the nominal parameter value $p_{nom} = 1.37$. For this parameter value one of its unstable equilibrium points is at $x^* = y^* = 0.8717$. In our simulations, maximum allowed parameter change is taken as $\delta p_{max} = 0.03$ and the radius of local control region is $\delta = 0.02$. The root mean square of one of the measured state is found as $x_{rms}^{Henon} = 1.327$.

5.1.3. The Lorenz System

The Lorenz system is a three-dimensional continuous-time chaotic system governed by the equations,

$$\begin{aligned} \dot{x} &= \sigma(y - x) \\ \dot{y} &= (\rho x - y - xz) \\ \dot{z} &= (xy - \beta z) \end{aligned} \tag{4.13}$$

where σ, ρ, and β are the system parameters. The nominal values $\sigma = 10$, $\rho = 28$, and $\beta = 8/3$ constitute the most investigated parameter set corresponding to chaotic behaviour. In simulations, for both real coordinates and delay coordinates, maximum allowed parameter change is chosen as $\delta\sigma_{max} = 0.30$ and the radius of local control region as $\delta = 0.30$. In general, the Poincaré surface can be chosen arbitrarily provided that it cuts the unstable periodic orbit under consideration. Here it is taken as a surface with $y = 8.4853$ with a downwards piercing direction, i.e. $\dot{y} < 0$. In real coordinates, the root mean square of one

of the measured state is $x_{rms}^{Lorenz} = 13.43$, while in the delay coordinates, the root mean square of measured delay coordinate is $y_{rms}^{Lorenz} = 2.675$, In the latter case 3 delay coordinates have been used with a delay time T = 100 ms.

5.1.4. The Double Rotor Map

The Double-Rotor map is a four-dimensional discrete-time chaotic system obtained as the Poincaré map of a 4-dimensional continuous-time, non-autonomous system. The dynamic equations of the Double-Rotor map are as follows:

$$\begin{bmatrix} X(k+1) \\ Y(k+1) \end{bmatrix} = \begin{bmatrix} \underline{\underline{M}}Y(k) + X(k) \\ \underline{\underline{L}}Y(k) + G(X(k)) \end{bmatrix} \tag{4.14}$$

where

$$X(k) = \begin{bmatrix} x_1(k) \\ x_2(k) \end{bmatrix} \in S^1 \times S^1, Y(k) = \begin{bmatrix} y_1(k) \\ y_2(k) \end{bmatrix} \tag{4.15}$$

$$G(X(k)) = \begin{bmatrix} c_1 \sin(x_1(k)) \\ c_2 \sin(x_2(k)) \end{bmatrix} \tag{4.16}$$

$$\underline{\underline{M}} = \begin{bmatrix} 0.48 & 0.21 \\ 0.21 & 0.69 \end{bmatrix}, \underline{\underline{L}} = \begin{bmatrix} 0.24 & 0.27 \\ 0.27 & 0.51 \end{bmatrix} \tag{4.17}$$

S^1 is the circle R (mod 2π). The constants c_1 and c_2 are given by $c_i = f_0 l_i$, where $f_0 = 9$, $l_1 = 1/\sqrt{2}$ and $l_2 = 1$ (Refer to (Romeiras *et al.*, 1992) for further details). For $f_0 = 9$, the map possesses two positive Lyapunov exponent, which implies hyper-chaotic behaviour. In the simulations, among others the equilibrium point $\begin{bmatrix} x_1^* & x_2^* & y_1^* & y_2^* \end{bmatrix}^T = [4.8719 \quad 2.3688 \quad -4.5547 \quad 10.3743]$ is chosen as the target, and maximum and minimum parameter values are taken as $f_{max} = 10$, $f_{min} = 8.9$ respectively and the radius of local control region is $\delta = 0.1$.

5.2 Simulation Results

Table 5.1 summarises the performances of OGY, AMC-I and AMC-II methods for the different chaotic systems under investigation.

The OGY method implemented here corresponds to the basic OGY algorithm where the coefficient matrices of the local linear model are calculated from the training data by the least square error approach. The maximum tolerable percentage noise is defined as the maximum amount of white noise (as a percentage of the root-mean-square value of the measured state), which can be added to the state measurements without endangering the stabilisation of the target. The table also shows the average waiting times under noisy conditions.

From Table 5.1 it can be observed that for the optimal number of extended control regions AMC-II provides better results than AMC-I with respect to average waiting time both with and without measurement noise. Although in both versions of AMC on-line phase is the same, this performance improvement is the result of the difference between approaches used in identification of control regions.

As illustrated in figure 4.3 and 4.4, in the first version, it is assumed that system can be steered into a lower level control region if and only if that region has the same control parameter value index with the previous one, which is not the case for the second version.

In AMC-II, basic assumption is that, system can be steered to the OGY region with properly chosen parameter perturbation from three different possible values, which are p_{min}, p_{nom} or p_{max}. As a result, these regions, which are different from the regions of the previous version, are modelled more accurately than before, which can be observed from Table 5.1 except for Lorenz system with delay coordinates. In this case, AMC-I gives the best performance in terms of average waiting time (number of piercing of Poincaré surface) but this performance can be different for different choice of Poincaré surface and delay time.

On the other hand, Table 5.2 shows the results obtained for the same chaotic systems by ECR methods as explained in section 4.2. Although ECR gives better results than our proposed method, AMC method does not require any additional computational cost, except the data gathering process, such as training time. Especially in Logistic and Hénon maps, AMC methods show quite reasonable performance levels, although there is no modelling tool such as neural networks. Also it has to be mentioned that, the required memory size is also smaller in AMC methods. Since parameters such as weights of neurons of the neural networks assigned to each an every cluster in ECR methods require more memory size than AMC methods. It can be seen as a trade-off between cost and performance of the targeting task.

Furthermore, robustness against measurement noise has been observed from results. This property of AMC methods is the result of analytical descriptions for the clusters and can be explained as follows: Since clusters are represented as hyper-ellipsoids in terms of their means and covariance matrices, expected effects of addition of some white noise are minimised by the stability of these statistical quantities against measurement noise.

Figure 5.1 shows the values of the system state and applied parameter values during the realisation of the targeting and control task for Logistic Map with 3 clustered control regions by AMC-II Method.

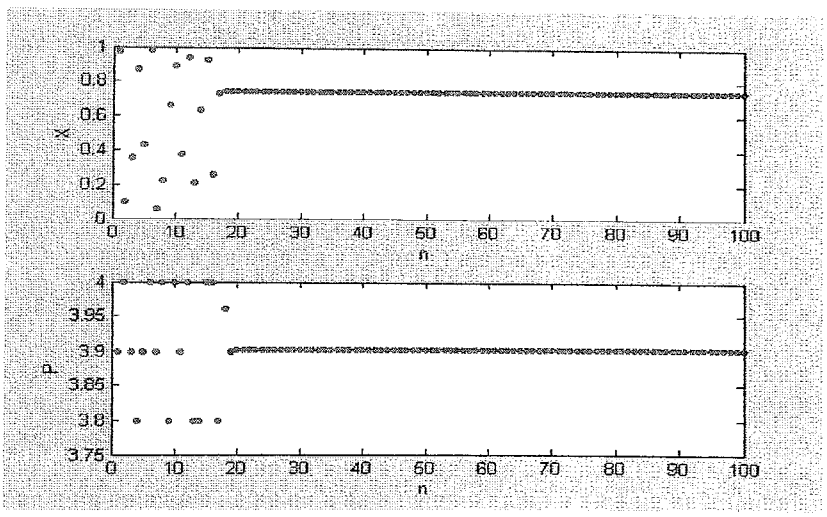

Figure 5.1 Application of the AMC-II Method to the Logistic map with 3 clustered control regions

Table 5.1. Comparison of OGY control and different versions of AMC methods for different chaotic systems

CHAOTIC SYSTEMS	*OGY*	*I*	*II*	*I*	*II*	*I*	*II*	*I*	*II*	*I*	*II*	*I*	*II*	*I*	*II*	*I*	*II*	*I*	*II*	*I*	*II*
# of control regions	**0**	**1**		**2**		**3**		**4**		**5**		**6**		**7**		**8**		**9**		**10**	
LOGISTIC MAP																					
Av. waiting time (without noise)	142.8	82.8	46.9	79.8	33.5	63.4	12.6	144.1	17.7	71.7	27.3	105.3	25.8	68.5	50.2	58.08	84.5	-	-	-	-
Av. waiting time (with 0.30% noise)	151.5	122.8	41.8	80.5	29.1	77.1	11.9	84.0	20.9	54.4	28.1	110.9	29.9	68.3	48.2	52.21	68.3	-	-	-	-
Online Response Time (Flops)		28	29	74	85	124	145	214	240	255	274	279	309	304	344	324	379	-	-	-	-
Memory Usage (Bytes)		80	80	224	256	384	448	672	752	800	864	880	976	960	1088	1024	1200	-	-	-	-
HENON MAP																					
Av. waiting time (without noise)	791.8	680.5	419.6	529.4	161.3	290.2	97.2	209.3	69.2	177.8	55.1	274.1	48.1	224.6	33.9	215.4	39.7	210.7	36.91	190.1	37.9
Av. waiting time (with 0.22% noise)	827.4	632.6	411.6	564.3	160.9	300.9	91.7	241.7	71.6	153.0	62.4	106.7	52.7	118.2	35.8	122.0	46.7	171.2	41.2	127.2	42.4
Online Response Time (x 10^3 Flops)		0.073	0.055	0.192	0.232	0.312	0.392	0.464	0.577	0.634	0.788	0.804	0.991	1.212	1.235	1.518	1.915	1.909	2.283	2.769	2.651
Memory Usage (Bytes)		192	144	528	528	864	912	1296	1344	1776	1872	2256	2352	3408	2976	4272	3600	5376	4272	6720	4944
LORENZ (Real Coord.)																					
Av. waiting time (without noise)	19.89	19.31	17.82	18.55	18.81	18.03	17.45	18.61	19.59	19.10	20.01	18.71	19.45	19.22	19.58	18.27	19.90	18.58	18.94	18.96	19.85
Av. waiting time (with 0.08% noise)	22.27	19.22	18.20	18.25	18.99	17.43	17.48	17.71	16.94	18.19	19.43	18.98	18.13	18.77	19.28	19.73	19.77	17.73	18.73	17.48	20.06
Online Response Time (x 10^3 Flops)		0.277	0.275	0.824	0.810	1.407	1.246	1.888	1.665	2.418	2.259	2.881	3.167	3.378	3.785	4.456	4.464	5.626	5.016	6.310	5.550
Memory Usage (Bytes)		768	624	2016	1632	3456	2593	4608	3456	5856	4704	6960	5952	8160	7104	9456	8304	10656	9312	11952	10320
LORENZ (Delay Coord.)																					
Av. waiting time (without noise)	36.18	21.04	26.27	19.82	25.56	19.91	26.01	23.57	25.64	25.70	26.01	29.14	27.41	27.53	27.24	27.85	27.31	26.81	26.73	25.37	25.93
Av. waiting time (with 0.36% noise)	37.02	23.83	30.06	20.50	26.07	19.88	26.93	26.03	29.39	25.42	29.17	26.00	26.24	26.92	27.57	28.42	29.48	26.60	28.90	29.09	28.96
Online Response Time (x 10^4 Flops)		.0612	.0418	.1917	.1181	.3910	.1862	.5455	.2765	.6838	.3500	.8229	.4142	.9813	.4802	1.126	.5471	1.278	.6152	1.423	.6794
Memory Usage (Bytes)		1728	1152	4992	2784	9312	4512	12960	6624	16320	8544	19680	10368	23424	12096	26880	13632	30528	15168	33984	16704
DOUBLEROTOR MAP																					
Av. waiting time (without noise)x10^5	4.46	4.37	3.84	2.45	0.86	1.57	0.59	0.81	0.64	0.62	4.82	0.42	5.29	1.33	5.40	1.89	4.68	2.36	5.67	2.40	5.05
Av. waiting time (with 0.27% noise)	4.90	3.60	4.07	3.51	0.87	2.37	0.60	1.23	0.52	0.64	4.86	0.57	5.19	1.90	5.40	1.98	4.87	3.18	5.46	3.89	5.02
Online Response Time (x 10^4 Flops)		.0150	.0150	.0731	.0697	.1334	.2088	.2557	.3141	.4113	.4221	.5916	.5358	.7443	.6600	.9387	.7785	1.1140	.9027	1.3237	1.0080
Memory Usage (Bytes)		640	480	2240	2080	4000	5600	7360	8480	11520	11360	16480	14400	20640	17760	25920	20960	30560	24320	36480	27200

Table 5.2. Comparison of the OGY control and various ECR methods for different chaotic systems (taken from [43])

LOGISTIC Map	**OGY**	**ECR-I**	**ECR-II**	**C-ECR-II**	**ECR-II**	**C-ECR-II**	**ECR-II**	**C-ECR-II**	**ECR-II**	**C-ECR-II**	**ECR-II**	**C-ECR-II**	**ECR-II**	**C-ECR-II**
# of activation regions	*0*	*2*	*1*		*2*		*3*		*4*		*5*		*6*	
Training time (flops)	$0.16\ 10^6$	$35\ 10^6$	$2.89\ 10^6$	$3.56\ 10^6$	$4.05\ 10^6$	$3.73\ 10^6$	$5.33\ 10^6$	$3.96\ 10^6$	$6.72\ 10^6$	$4.07\ 10^6$	$6.76\ 10^6$	$4.18\ 10^6$	$8.06\ 10^6$	$4.21\ 10^6$
Av. Wait. t. (without noise)	*143.7*	*50.87*	*51.31*	*58.571*	*46.37*	*53.027*	*13.75*	*8.575*	*9.32*	*5.753*	*9.23*	*5.316*	*9.14*	*5.523*
Av. Wait. t. (with 0.30% noise)	*156.8*	*52.64*	*52.96*	*58.153*	*46.99*	*52.797*	*14.16*	*8.694*	*10.96*	*5.894*	*11.26*	*5.418*	*11.25*	*5.747*
HENON Map	**OGY**	**ECR-I**	**ECR-II**	**C-ECR-II**	**ECR-II**	**C-ECR-II**	**ECR-II**	**C-ECR-II**	**ECR-II**	**C-ECR-II**	**ECR-II**	**C-ECR-II**	**ECR-II**	**C-ECR-II**
# of activation regions	*0*	*3*	*3*		*4*		*5*		*6*		*7*		*8*	
Training time (flops)	$0.92\ 10^6$	$601\ 10^6$	$33\ 10^6$	$28.4\ 10^6$	$35\ 10^6$	$29.2\ 10^6$	$42\ 10^6$	$29.8\ 10^6$	$48\ 10^6$	$30.5\ 10^6$	$56\ 10^6$	$31.0\ 10^6$	$57\ 10^6$	$31.6\ 10^6$
Av. Wait. t. (without noise)	*767.9*	*108.73*	*107.18*	*121.76*	*101.72*	*89.56*	*59.89*	*57.95*	*30.06*	*27.89*	*21.94*	*17.17*	*22.50*	*15.39*
Av. Wait. t. (with 0.22% noise)	*837.8*	*134.9*	*126.00*	*108.58*	*104.82*	*82.56*	*60.25*	*57.59*	*39.29*	*26.52*	*31.00*	*15.51*	*30.65*	*13.64*
LORENZ Syst. (real coord.)	**OGY**	**ECR-I**	**ECR-II**	**C-ECR-II**	**ECR-II**	**C-ECR-II**	**ECR-II**	**C-ECR-II**	**ECR-II**	**C-ECR-II**	**ECR-II**	**C-ECR-II**	**ECR-II**	**C-ECR-II**
# of activation regions	*0*	*1*	*1*		*2*		*3*		*4*		*5*		*6*	
Training time (flops)	$0.21\ 10^6$	$96\ 10^6$	$443\ 10^6$	49.910^6	$454\ 10^6$	$50.6\ 10^6$	$455\ 10^6$	$51.1\ 10^6$	$455\ 10^6$	$51.4\ 10^6$	$456\ 10^6$	$51.5\ 10^6$	$456\ 10^6$	$51.5\ 10^6$
Av. Wait. t. (without noise)	*15.09*	*6.64*	*6.14*	*6.80*	*6.43*	*6.44*	*6.45*	*6.43*	*6.57*	*6.39*	*6.45*	*6.42*	*6.66*	*6.42*
Av. Wait. t. (with 0.08% noise)	*18.91*	*6.81*	*6.43*	*7.93*	*6.02*	*7.79*	*6.34*	*7.49*	*5.93*	*6.82*	*5.92*	*6.65*	*6.86*	*6.59*
LORENZ Syst. (delay coord.)	**OGY**	**ECR-I**	**ECR-II**	**C-ECR-II**	**ECR-II**	**C-ECR-II**	**ECR-II**	**C-ECR-II**	**ECR-II**	**C-ECR-II**	**ECR-II**	**C-ECR-II**	**ECR-II**	**C-ECR-II**
# of activation regions	*0*	*1*	*1*		*2*		*3*		*4*		*5*		*6*	
Training time (flops)	$0.24\ 10^6$	$5.91\ 10^{10}$	$4.81\ 10^9$	$0.84\ 10^9$	$4.84\ 10^9$	$0.87\ 10^9$	$4.86\ 10^9$	$0.88\ 10^9$	$4.87\ 10^9$	$0.89\ 10^9$	$4.88\ 10^9$	$0.89\ 10^9$	$4.89\ 10^9$	$0.89\ 10^9$
Av. Wait. t. (without noise)	*35.32*	*18.31*	*17.92*	*16.21*	*13.62*	*14.90*	*12.83*	*14.02*	*12.76*	*12.23*	*12.73*	*12.61*	*12.73*	*12.47*
Av. Wait. t. (with 0.36% noise)	*34.20*	*20.08*	*18.93*	*15.37*	*15.31*	*15.48*	*14.21*	*12.94*	*15.24*	*11.67*	*15.26*	*11.70*	*15.22*	*11.25*
DOUBLE ROTOR MAP	**OGY**	**ECR-I**	**ECR-II**	**C-ECR-II**	**ECR-II**	**C-ECR-II**	**ECR-II**	**C-ECR-II**	**ECR-II**	**C-ECR-II**	**ECR-II**	**C-ECR-II**	**ECR-II**	**C-ECR-II**
# of activation regions	*0*		*1*		*2*		*3*		*4*		*5*		*6*	
Training time (flops)	$1.92\ 10^6$	-	$13.5\ 10^6$	$24.7\ 10^6$	$13.5\ 10^6$	$27\ 10^6$	$15.5\ 10^6$	$31.8\ 10^6$	$16.9\ 10^6$	$33.9\ 10^6$	$16.9\ 10^6$	$35.5\ 10^6$	$17.4\ 10^6$	$36.5\ 10^6$
Av. Wait. t. (without noise)	*394000*	-	*70447*	*57893*	*8886*	*11614*	*7281*	*1238*	*7501*	*1288*	*6570*	*1484*	*6242*	*1474*
Av. Wait. t. (with 0.27% noise)	*394000*	-	*66382*	*50537*	*9815*	*10661*	*7081*	*1101*	*6859*	*937*	*6229*	*1022*	*6670*	*1005*

6. CONCLUSION

In this thesis, a method has been developed, which allows the application of the Clustered-ECR-II targeting method using simple analytical models rather than artificial neural networks. Both variants of the proposed method, AMC-I and AMC-II maintain the basic assumptions of the OGY control.

The main advantage of this method is the fact that, it uses very simple models of the system dynamics in a larger portion of the phase. The analytical description of the regions in terms of hyper-ellipsoids results in very small computational memory usage. AMC methods maintain some desirable properties of the ECR targeting method like small control power expenditure and applicability to high dimensional chaotic systems and delay coordinates. On the other hand, the employment of simple analytical models in AMC methods requires some additional restriction, namely the usage of finite number of discrete values of the control parameter instead of continuous parameter variations and single control parameter usage.

In this thesis simulations have been performed on dissipative chaotic systems using single control parameter with three discrete allowable values. This restriction reduces the coverage of the phase space by control regions and results in a longer average waiting time compared to the Clustered-ECR-II method. The average waiting time can be reduced by increasing the number of control parameters and the number of allowed values of the control parameter(s). This, however, will increase the computational burden. Hence, the number of allowed values of the control parameter has to be determined considering the trade-off between targeting speed and computational burden.

The simplicity of the data gathering process allows some successive trial and error iterations for optimisation of some controller parameters like the radius of the OGY region, the clustering radius etc.

The clustering algorithm employed both in Clustered-ECR-II and AMC methods is a very simple one. The usage of a more sophisticated clustering algorithm can improve the average waiting time in all these methods while increasing the computational burden.

REFERENCES

1. Lorenz E.N., "Deterministic non-periodic flow", J. Atmos. Sci., Vol. 20, pp. 130-141, 1963.

2. Ott E., C. Grebogi and J.A. Yorke, "Controlling Chaos", Physical Review Letters, Vol. 64, pp. 1196-1199, 1990.

3. Strogatz, S.H., *Nonlinear Dynamics and Chaos: With Applications in Physics, Biology,Chemistry, and Engineering*, Addison-Wesley 1995.

4. Wiggins S., *Introduction to Applied Nonlinear Dynamical Systems and Chaos*, Springer, Berlin, 1996.

5. Devaney R.L., *An Introduction to Chaotic Dynamical Systems*, Addison-Wesley, 1987.

6. Poincaré H., *Les Méthodes Nouvelles de la Mécanique Céleste*, Gauthier- Villars, Paris, 1899.

7. Lathrop D. and E. Kostelich, "Characterization of an experimental strange attractor by periodic orbits", Physical Review A, Vol. 40, pp. 4028-4031, 1989.

8. Slotine J. J. and W. Li., *Applied Nonlinear Control*, Prentice-Hall, 1991.

9. Tsonis A., *Chaos: From Theory to Applications*, Plenum Press, New York, 1992.

10. Abarbanel, H., R. Brown, J.J. Sidorowich and L.S. Tsimring, "Rev. of Modern Physics", Vol. 65, No. 4, pp. 1331-1392, 1993.

11. Takens F., "Dynamical Systems and Turbulance", Lecture Notes in Mathematics, Springer Verlag, New York, 1981.

12. Boccaletti S., C. Grebogi, Y.C. Lai, H. Mancini and D. Maza, "The Control of Chaos: Theory and Applications", Physics Reports, Vol. 329, pp. 103-197, 2000.

13. Barreto E. and C. Grebogi, "Multi-parameter Control of Chaos", Physical Review E, Vol. 52, pp. 3553-3557, 1995.

14. Nitsche G. and U. Dressler, "Controlling Chaotic Dynamical Systems Using Time Delay Coordinates", Physica D, vol. 58, pp. 153-164, 1992.

15. So P. and E. Ott, "Controlling Chaos Using Time Delay Coordinates via Stabilization of Periodic Orbits", Physical Review E, Vol. 51, pp. 2955-2962, 1995.

16. Romeiras F., C. Grebogi, E. Ott and W. Dayawansa, "Controlling Chaotic Dynamical Systems", Physica D, Vol. 58, pp. 165-192, 1991.

17. Hong Z., Y. Jie, W. Jiao and W. Yinghai, "General Method of Controlling Chaos", Physical Review E, Vol. 53, pp. 299-306, 1996.

18. Ding M., W. Yang, V. In, W. Ditto, M. Spano and B. Gluckman, "Controlling Chaos in High Dimensions: Theory and Experiment", Physical Review E, Vol. 53, pp. 4334-4344, 1996.

19. Hunt E., "Stabilizing High-period Orbits in a Chaotic System: The Diode Resonator", Physical Review Letters, Vol. 67, pp. 1953-1955, 1991.

20. Carr T. and I. Schwartz, "Controlling Unstable Steady States Using System Parameter Variation and Control Duration", Physical Review E, Vol. 50, pp. 3410-3415, 1994.

21. Schuster H. and E. Niebur, "Parametric Feedback Resonance in Chaotic Systems", Physical Review Letters, Vol. 76, pp. 400-403, 1996.

22. Schwartz I., T. Carr and I. Triandaf, "Tracking Controlled Chaos: Theoretical Foundations and Applications", Chaos, Vol. 7, pp. 664-679, 1997.

23. Bielawski S., D. Derozier and P. Glorieux, "Experimental Characterization of Unstable Periodic Orbits by Controlling Chaos", Physical Review A, Vol. 47, pp. R2492-R2495, 1993.

24. Bielawski S., D. Derozier and P. Glorieux, "Controlling Unstable Periodic Orbits by a Delayed Continuous Feedback", Physical Review E, Vol. 49, pp. R971-R974, 1994.

25. Shinbrot T., E. Ott, C. Grebogi and J. A. Yorke, Physical Review Letters, Vol.65, pp. 3215, 1990.

26. Shinbrot T., E. Ott, C. Grebogi and J. A. Yorke, Physical Review A, Vol. 45, pp. 4165, 1992.

27. Shinbrot T., W. Ditto, C. Grebogi, E. Ott, M. Spano and J. A. Yorke, Physical Review Letters, Vol. 68, pp. 2863, 1992.

28. Kostelich E.J., C. Grebogi, E. Ott and J. A. Yorke, Physical Review E, Vol. 47, pp. 305, 1993.

29. Barreto E., E. Kostelich, C. Grebogi, E. Ott and J. A. Yorke, Physical Review E, Vol. 51, pp. 4169, 1995.

30. Glass K., M. Renton, K. Judd and A. Mees, Physics Letters A, Vol. 203, pp. 107, 1995.

31. Paskota M., A. I. Mees and K. L. Teo, Int. J. of Bif. and Chaos, Vol. 5, pp. 573, 1995.

32. Paskota M., A. I. Mees and K. L. Teo, Int. J. of Bif. and Chaos, Vol. 5, pp. 1167 1995.

33. Paskota M., A. I. Mees and K. L. Teo, Dynamics and Control, Vol. 7, pp. 25, 1997.

34. Lee H.W.J., M. Paskota and K. L. Teo, Int. J. of Bif. and Chaos, Vol. 7, pp. 607, 1997.

35. Paskota M. and H. W. J. Lee, Chaos, Solitons and Fractals, Vol. 8, pp. 1533, 1997.

36. Cao L., K. Judd and A. Mees, Physics Letters A, Vol. 231, pp. 367, 1997.

37. Baptista M., Int. J. of Bif. and Chaos, Vol. 8, pp. 1575, 1998.

38. Gadaleta S. and G. Dangelmayr, "Optimal Chaos Control Through Reinforcement Learning", Chaos Vol. 9, pp. 775-788, 1999.

39. İplikci S., *A Neural Network Based Local Control and Targeting Method for Chaotic Dynamics*, M.S. Thesis, Bogazici University, Turkey, 1999.

40. İplikci S. and Y. Denizhan, "Control of Chaotic Systems Using Targeting By Extended Control Regions Method", *Third International Conference on Computing Anticipatory Systems (CASYS 1999)*, AIP Conf. Proc. Vol. 517, pp. 453, 1999.

41. Sütcü Y., S. İplikci and Y. Denizhan, "Improvement of Targeting Efficiency in Chaos Control Using Clustering", *Fifth International Conference on Computing Anticipatory Systems (CASYS 2001)*, Liège, Belgium, August 13-18, 2001.

42. Jain A.K., M.N. Murty and P.J. Flynn, "Data Clustering: A Review", ACM Computing Surveys, Vol. 31, No. 3, September 1999.

43. İplikci S., *Computationally Intelligent Techniques for Stabilisation and Targeting of Chaotic Systems*, PhD. Thesis, Bogazici University, Turkey, 2002.